1963

Rectilinear oscillations of a sphere immersed in a bounded viscous fluid

Kenneth George McConnell
Iowa State University

McCONNELL, Kenneth George, 1934–
RECTILINEAR OSCILLATIONS OF A SPHERE IMMERSED IN A BOUNDED VISCOUS FLUID.

Iowa State University of Science and Technology
Ph.D., 1963
Engineering Mechanics

RECTILINEAR OSCILLATIONS OF A SPHERE IMMERSED

IN A BOUNDED VISCOUS FLUID

by

Kenneth George McConnell

A Dissertation Submitted to the

Graduate Faculty in Partial Fulfillment of

The Requirements for the Degree of

DOCTOR OF PHILOSOPHY

Major Subject: Theoretical and Applied Mechanics

Approved:

Signature was redacted for privacy.

In Charge of Major Work

Signature was redacted for privacy.

Head of Major Department

Signature was redacted for privacy.

Dean of Graduate College

Iowa State University
Of Science and Technology
Ames, Iowa

1963

TABLE OF CONTENTS

INTRODUCTION

The steady motion of a rigid body in a fluid has been studied in great detail, and the results of both theoretical and experimental investigations are generally well known. The unsteady motion of a rigid body in a fluid has been subjected to few studies. The conflicting or inconclusive information in the available literature makes it difficult to analyse problems of unsteady motion.

The objectives of this study were (1) to examine the theoretical equations governing the behavior of a rigid body oscillating with rectilinear oscillations relative to a bounded viscous fluid which may also have rectilinear motion independent of the rigid body, (2) to develop a suitable experimental technique for investigating problems of this type, and (3) to determine if a suitable parameter or set of parameters exist which can serve as a guide or guides for predicting whether viscous effects are significant. Both motion of the fluid and of the rigid body are unsteady in this type of problem.

A. The Phenomenon

As a simple example to illustrate the major difference between steady and unsteady motion of a rigid body, consider a body of unit mass to be in equilibrium and at rest in the absence of a fluid. Apply a unit force to the body. The result, according to Newton's second law, is a unit acceleration. Now, place the same body in a fluid where it is in equilibrium and at rest. By applying a unit force, the resulting acceleration has been observed to be less than unity. The only difference is the presence of the fluid. "Fluid drag", as it is usually defined, is dependent on the velocity and the presence of viscosity. When the body starts from rest, the velocity and hence, the "fluid drag" are zero. Therefore, the drag is not the property of the fluid that causes this discrepency.

When the body moves through the field, the fluid must move out and in to let the body pass. The faster the body moves the more rapidly the fluid must move out and in. This implies that the fluid velocity at any fixed distance from the body is proportional to the velocity of the body and that the kinetic energy of the fluid is changed by the forces of the body on the fluid.

It can be shown that the kinetic energy, T, of the fluid at any instant is related to the mass of fluid displaced by the body and to the velocity of the body. If the velocity of the fluid is known at every point, this relationship is given by

$$T = \frac{\rho}{2}\int^{\text{Vol.}} v^2 \quad dV = \frac{kM}{2} U^2$$

where v is the velocity of the fluid at the point, dV is the differential volume, k is the added mass coefficient which depends on the geometry of the body and several fluid properties, M is the mass of fluid dispaced by the body, and U is the velocity of the body. Let F be the external force applied to the body in its direction of motion. The rate at which the external work is done on the system by the force F must equal the time rate of change of the kinetic energy for a conservative (ideal fluid) system, so that

$$FU = \frac{dT}{dt} = (m + kM) \quad U \frac{dU}{dt}$$

or

$$F = (m + kM) \frac{dU}{dt}$$

where m is the mass of the body. From the last expression, it is seen that the mass of the body is increased by the term kM which is called the added mass. This term affects the motion of the body but does not alter its weight.

In steady flow the term $kM \frac{dU}{dt}$ is not present. Thus, by considering an ideal case where "fluid drag" is not present, it is seen that the acceleration of the unit mass should be less than unity due to the change in the velocity of the fluid necessary to let the body pass more rapidly.

An interesting insight into what occurs in this phenomena is given by Darwin (7) who considered the path followed by a given particle of an ideal fluid when a body passes a given point in space near this particle. He shows that the particle will take on a net displacement in the direction of motion of the body when the body passes the given point in space. The mass of fluid which is displaced in the direction of motion of the body is exactly equal to the mass of fluid contained in a volume equal to that of the body when the body passes this point in space. Imlay (13) clarifies this by saying, "Although ... the added mass ... "is" proportional to the mass ... of this specific volume of fluid, the mistake must not be made of assuming that the added mass effects involve only a limited volume of fluid, or that some limited volume of fluid moves with the body - the so-called 'entrained fluid' erroneously described by some authors. All the particles of fluid move, although the motion of the fluid is more pronounced in the neighborhood of the body. Darwin has endeavored to describe the nature of this motion." It should be noted that Imlay's statement is for an ideal fluid. In a real fluid, a small amount of fluid is dragged with the body due to the presence of viscosity which is not accounted for in Darwin's solution. This small quantity adds to the values predicted from the analysis of a conservative system.

Three useful methods are generally available for solving fluid mechanics problems. These are:

1. Potential flow theory in which the fluid is considered to be ideal; that is, no shearing stresses may be created in the fluid and the fluid moves irrotationally. This is the simplest analytical method.

2. Real fluid flow theory in which shearing stresses do exist in the fluid. Solutions based on this theory are generally difficulty to obtain since the equations governing the fluid motion contain non-linear terms. If the non-linear terms do not drop out due to the boundary conditions and continuity relationships, a solution can sometimes be obtained by simply neglecting these terms. This type of solution is commonly called the <u>viscous</u> or <u>slow</u> flow solution since the viscous forces are considered to be predominant.

3. A solution based on an experimental program.

When these three methods are combined, the first method gives a solution of the fluid behavior when the viscous forces are not important. The second (viscous flow) method gives a solution when the viscous forces are predominant. The third method provides a means to supplement the first two, indicate their range of validity, and provides a solution between these two extremes. These three methods are employed to accomplish the objectives of this study.

The geometry of the system enters into each of the methods. Hence, a given geometry had to be selected which would show the effects of viscosity as well as permit a theoretical solution. Two simple geometries were available; i.e., two concentric spheres and two concentric cylinders.

Stokes (29, 30) and (31, 32) has solved the concentric cylinder problem for an infinite fluid medium and the concentric sphere problem by using both (the potential and the viscous flow) methods. The concentric cylinder solution is developed for infinitely long cylinders. This introduces additional complications for experimental work. Thus, the concentric spheres were selected as most useful in trying to accomplish the objectives.

The terminology used in the literature is confusing. Imlay (13) described the situation accurately when he stated, "What the added mass phenomenon is, and what terms should be used to represent it in equations of motion do not appear to be understood clearly by many persons. Clarity has not been enhanced, furthermore, by the variety of names, such as 'virtual mass', 'ascension to mass', 'apparent mass', and 'hydrodynamic mass' applied to the phenomenon." Induced mass and equivalent mass can be added to Imlay's list. In order to clarify the meaning of these names, the following definitions are usually used. Added mass, apparent mass, induced mass and hydrodynamic mass are usually defined as the mass which affects the motion of the body without increasing its weight. Virtual mass and equivalent mass are usually defined as the sum of the mass of the body and the added mass. Added mass or hydrodynamic mass and virtual mass are predominate terms used in contemporary literature. The preceding definitions are used throughout the thesis.

B. Survey of Literature

This survey of literature is limited to material concerned with spheres. A complete historical sketch and bibliography on added mass for other shapes as well as spheres is given by Stelson (27).

The first observation of the phenomenon of added mass is credited to DuBaut (8) between 1779 and 1786. His observations on spherical pendulum bobs in water were completely overlooked until 1826 when Bessel (4) rediscovered the added mass effect with similar experiments on pendulum bobs in air. Bessel's experiments caused considerable excitement in England since the Royal Navy out of scientific interest had measured the periods of pendulums all over the world. Sabine (25) in 1829 and Baily (1) in 1832 published their experimental results. The values obtained for spherical pendulum bobs in these early experiments ranged from 0.45 to 0.67 for DuBaut with an average of 0.585, 0.625 to

0.956 for Bessel, 0.655 for Sabine, and 0.834 for Baily. The potential solution for an infinite medium gives a value of 0.50.

McEwen (17) in 1911 attempted to check Stokes' (31, 32) viscous flow solution in an infinite medium. He used water and a very heavy oil. The results indicated fairly good agreement with the viscous solution. Krishnayer (15) in 1923 conducted experiments similar to McEwen's in a viscous infinite fluid with three spheres of different sizes. His experimental values were consistently one percent high. This may be due to the close proximity of the fluid surface and the driving magnets of his experimental apparatus. Valensi (35) in 1952 studied the oscillations of a sphere in an infinite medium. He concluded Stokes' viscous solution was only good for small amplitudes.

Cook (6) in 1920 studied this problem by dropping spheres into a large tank of water. He concluded that the added mass coefficient was about 0.46. Stelson (27, 28) in 1952 studied the added mass coefficient for many different shapes including spheres. His tests were conducted in a large tank of water at frequencies of about 10 to 30 cycles per second. The results were in good agreement with the potential flow solutions. He attempted to avoid viscous effects and did so successfully. Most of his results are within one percent of the theoretical solutions.

The early experimental work of DuBuat, Bessel, Sabine, and Baily indicated a need for a theoretical solution since the data were not in agreement. Green (10) made the first successful attempt in 1836 and states ".... it is not sufficient merely to allow for the loss of weight caused by the fluid medium, but that it will likewise be requisite to conceive the density of the body augmented by a quantity proportional to the density of the fluid. The value of the last quantity named, ..., has been completely determined..." for a spheroid in an infinite ideal fluid, and for the special case of a "..sphere is precisely equal to half the density of the surrounding fluid." Stokes (29, 30) and (31, 32) solved the problem of concentric spheres from the potential flow (in 1843) and the viscous flow (in 1850) standpoint. Meyer (19) in 1871 improved on Stokes' viscous solution by considering the effects of large amplitudes. This solution has not been verified experimentally.

Other theoretical work has been done by Hicks (12), Boussinesq (5), Basset (2) and (3), Rayleigh (24), Polya (23), Haberman (11), and Imlay (13).

The experimental results reported in the literature have often been conflicting or inconclusive. These studies have been too narrow since the viscous effects have been either avoided by using low viscosity fluids or studied over the limited range of a single viscous fluid. There is a need for a series of systematic experimental studies on unsteady rigid body motion in a viscous fluid which covers the entire spectrum from the viscous flow theory through the potential flow theory. There is a need to study the viscous effects on the equations of motion which will enhance the understanding of the added mass phenomenon. This study was conducted to clarify and further this understanding for the special case of rectilinear motion in a real fluid.

II. THEORETICAL ANALYSIS

The general character of the problem considered in this investigation (see the first objective in the introduction) may be obtained by considering body A of Fig. 1-a which is surrounded by a fluid. The fluid is contained inside the envelope B which has an absolute acceleration in the $\overline{X}$-direction. Body A is attached to the envelope B by an elastic spring and has an arbitrary external force F(t) acting on it. It is necessary to write the equation of motion of body A if the motion of body A is to be predicted. In order to carry out this task, let $\overline{X}$ locate the center of mass of body A, x_o locate the equilibrium position of A relative to B in the absolute reference system, and x be the displacement of A from its equilibrium position relative to B.

Figure 1-b is a free body diagram of the forces acting on body A. G(t) is the sum of the forces due to the fluid (both pressure and shearing stresses will contribute) integrated over the surface of body A. By taking to the right as positive and applying Newton's second law, the governing equation of motion is

$$m\,\overline{a}_x = -K'x + F(t) + G(t) \tag{1}$$

where $\overline{a}_x$ may be written as

$$\overline{a}_x = \frac{d^2\overline{X}}{dt^2} = \frac{d^2x_o}{dt^2} + \frac{d^2x}{dt^2}$$

which indicates that the absolute acceleration of body A may be written as two separate terms. The first term is the absolute acceler-

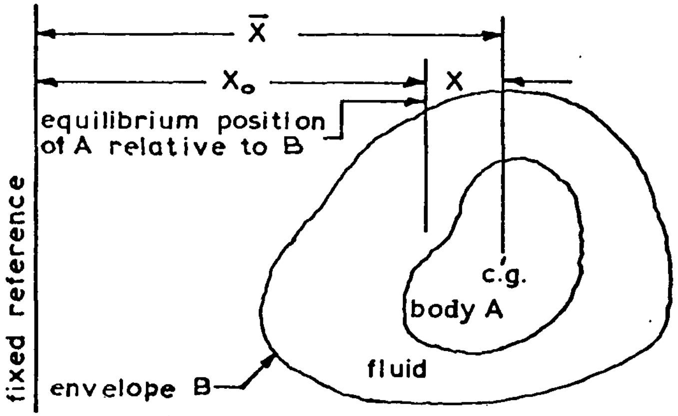

Fig. 1-a Generalized body locations

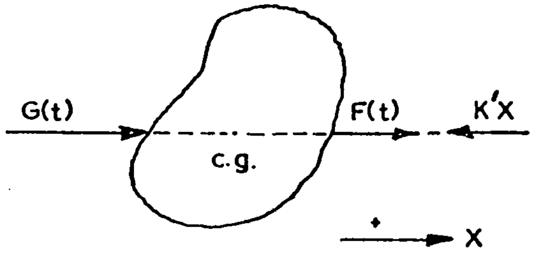

Fig. 1-b Free body diagram of body A

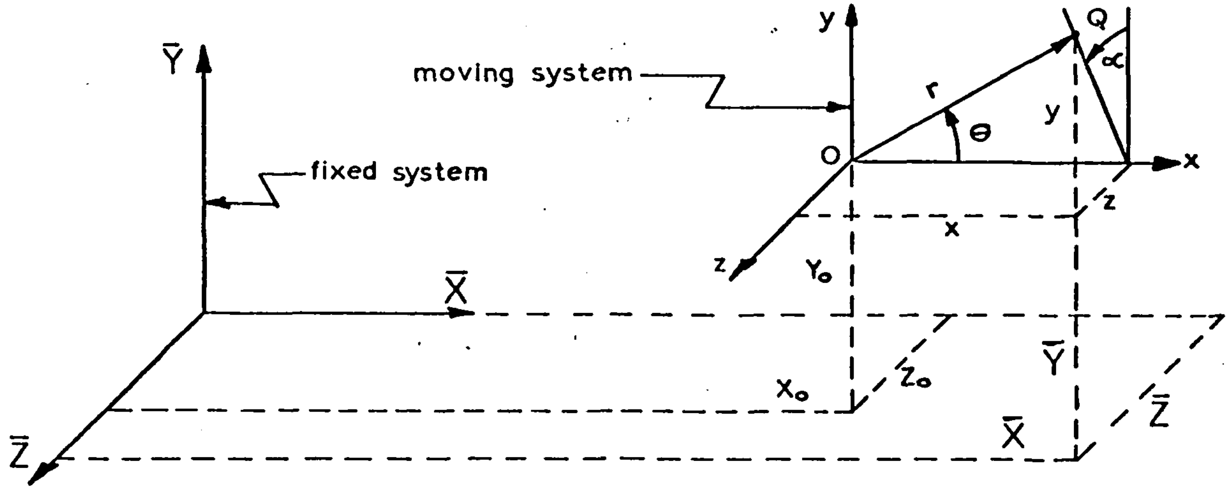

Fig. 2 Fixed and moving coordinate systems

ation of the envelope, and the second term is the relative acceleration of body A with respect to the envelope. By substituting this expression for $\bar{a}_x$ into Eq. 1, the equation may be written as

$$m \frac{d^2x}{dt^2} + K'x = - m \frac{d^2x_o}{dt^2} + F(t) + G(t) \tag{1-a}$$

The left-hand side of Eq. 1-a is a second-order differential equation written in terms of the displacement of body A relative to the envelope B while the first two terms on the right-hand side are arbitrary forcing functions. Before Eq. 1-a can be solved, it is necessary to determine the nature of the function G(t). Three methods (potential flow theory, viscous flow theory, and an experimental approach) are used to determine G(t) for the special case of concentric spheres.

The theoretical analysis for two concentric spheres with both the inner and outer spheres having rectilinear motion may be approached most easily by transforming the basic equations to a moving coordinate system. Subsequently, the potential flow solution will be worked out in some detail, and the viscous solution developed by Stokes (31, 32) will be outlined.

A. Transformation of Equations to Moving Coordinate System

1. Fixed and moving coordinate systems

In Fig. 2, Q is a point of fluid with coordinates of $\bar{X}$, $\bar{Y}$, $\bar{Z}$ in the fixed coordinate system and coordinates of x, y, z in the moving coordinate system. O is the origin of the moving coordinate system with coordinates of x_o, y_o, z_o in the fixed system. The moving coordinate system is allowed to translate in an arbitrary manner with respect to the fixed system, but it cannot rotate with respect to the fixed system. The moving spherical coordinate system r, θ, α is also shown in Fig. 2 for later reference.

a. Linear transformation of coordinates, velocities, and accelerations

The linear transformation between coordinates is

$$\begin{aligned} \bar{X} &= x_o + x \\ \bar{Y} &= y_o + y \\ \bar{Z} &= z_o + z \end{aligned} \tag{2-a}$$

and by differentiation of Eq. 2-a with respect to time, the linear transformation of velocities is

$$\begin{aligned} \bar{U} &= u_o + u \\ \bar{V} &= v_o + v \\ \bar{W} &= w_o + w \end{aligned} \tag{2-b}$$

The linear transformation of accelerations is obtained by differentiating Eq. 2-b with respect to time. This gives

$$\begin{aligned} \bar{a}_x &= \frac{d\bar{U}}{dt} = \frac{du_o}{dt} + \frac{du}{dt} \\ \bar{a}_y &= \frac{d\bar{V}}{dt} = \frac{dv_o}{dt} + \frac{dv}{dt} \\ \bar{a}_z &= \frac{d\bar{W}}{dt} = \frac{dw_o}{dt} + \frac{dw}{dt} \end{aligned} \tag{2-c}$$

b. Linear transformation of partial derivatives The transformation of the partial derivatives may be examined from two view points. First, consider two planes which are parallel to the $\overline{YZ}$ - plane. At a given instant of time, let these planes be located by $\overline{X}$ and $\overline{X} + d\overline{X}$ in the fixed coordinate system. The change in the absolute velocity $\overline{U}$, for example, that occurs between the two planes from a point at $(\overline{X}, \overline{Y}, \overline{Z})$ to a point at $(\overline{X} + d\overline{X}, \overline{Y}, \overline{Z})$ is given by $\frac{\partial \overline{U}}{\partial \overline{X}} d\overline{X}$. At this same instant of time, the change in the relative velocity between these same two points is given by $\frac{\partial u}{\partial x} dx$ since u_o is a common velocity of both points and x_o is a common distance to both points. Then, since $d\overline{X} = dx$ at a given instant of time, $\frac{\partial \overline{U}}{\partial \overline{X}}$ must be equal to $\frac{\partial u}{\partial x}$.

The second and more rigorous view point is to carefully note the definitions of the velocities, the coordinates of which they are functions, and the characteristics of the displacements at a given instant of time. These are:

$$\overline{U} = \overline{U}(\overline{X}, \overline{Y}, \overline{Z}) = \frac{d\overline{X}}{dt},$$

$$u_o = u_o(x_o, y_o, z_o) = \frac{dx_o}{dt},$$

$$u = u(x, y, z) = \frac{dx}{dt},$$

and

$$\overline{X} = x_o + x$$

where u_o is only dependent on the absolute coordinates which locate the origin of the moving coordinate system. Hence, u_o is independent of $\overline{X}$ and x.

Then,

$$\frac{\partial \bar{U}}{\partial \bar{X}} = \frac{\partial \bar{U}}{\partial x} \frac{dx}{d\bar{X}} = \frac{\partial u_o}{\partial \bar{X}} + \frac{\partial u}{\partial x} \frac{dx}{d\bar{X}} \quad \text{or}$$

$$\frac{\partial \bar{U}}{\partial \bar{X}} = \frac{\partial u}{\partial x} \tag{3}$$

since $d\bar{X} = dx$ and $\frac{\partial u_o}{\partial \bar{X}} = 0$. Similarly, the second partial derivative transforms as

$$\frac{\partial^2 \bar{U}}{\partial \bar{X}} = \frac{\partial^2 u}{\partial x^2} \tag{4}$$

With these relations, it is possible to transform the Navier-Stokes equations from the absolute to the moving coordinate system.

2. <u>Transformation of Navier-Stokes equations</u>

The Navier-Stokes equations are derived on the basis of several assumptions. These are:

1. The fluid is an incompressible continuum.
2. The shearing stresses are proportional to the rate of shearing strain.
3. The constant of proportionality between shearing stress and rate of shearing strain is independent of the pressure.

These assumptions are satisfied for most common liquids.

The Navier-Stokes equation governing the fluid motion in the $\bar{X}$-direction of the fixed coordinate system is

$$\rho \, \bar{a}_x = B_x - \frac{\partial P}{\partial \bar{X}} + \mu \, \bar{\nabla}^2 \, \bar{U} \tag{5}$$

where ρ is the density of the fluid, B_x is the body force acting in the positive $\overline{X}$-direction, μ is the absolute viscosity of the fluid, $\frac{\partial P}{\partial \overline{X}}$ is the pressure gradient in the $\overline{X}$ direction, and $\overline{\nabla}^2$ is the Laplacian operator in the fixed coordinate system. By virtue of Eq. 4, the Laplacian operator is seen to transform as

$$\overline{\nabla}^2 \quad \overline{U} = \nabla^2 u \tag{6}$$

from the fixed system to the moving system. By combining Eqs. 2-c, 3, 4, and 6, the Navier-Stokes equation in the moving coordinate system may be written as

$$\rho \frac{du}{dt} = (B_x - \rho \frac{du_o}{dt}) - \frac{\partial P}{\partial x} + \mu \nabla^2 u \tag{7}$$

where a hypothetical body force of $(B_x - \rho \frac{du_o}{dt})$ replaces the original body force in the fixed coordinate system. In a similar manner, the entire set of Navier-Stokes equations for the moving reference frame is easily derived, and these equations are

$$\rho \frac{du}{dt} = (B_x - \rho \frac{du_o}{dt}) - \frac{\partial P}{\partial x} + \mu \nabla^2 u \tag{7}$$

$$\rho \frac{dv}{dt} = (B_y - \rho \frac{dv_o}{dt}) - \frac{\partial P}{\partial y} + \mu \nabla^2 v \tag{7-a}$$

$$\rho \frac{dw}{dt} = (B_z - \rho \frac{dw_o}{dt}) - \frac{\partial P}{\partial z} + \mu \nabla^2 w \tag{7-b}$$

From Eqs. 7, 7-a, and 7-b, the solution of a moving coordinate system problem is reduced to solving these equations where the body force is changed by an "inertia" body force due to the acceleration of the moving coordinate system and the boundary conditions are those of the motion relative to the moving coordinate system. The Euler equations are the same as Eqs. 7, 7-a, and 7-b when the absolute viscosity (μ) is set equal to zero.

3. Transformation of the continuity equation

The continuity equation, as it is used in this problem, is based on a single assumption; that is, the fluid is an incompressible continuum. In the fixed coordinate system, the continuity equation is

$$\frac{\partial \overline{U}}{\partial \overline{X}} + \frac{\partial \overline{V}}{\partial \overline{Y}} + \frac{\partial \overline{W}}{\partial \overline{Z}} = 0$$

which transforms to

$$\frac{\partial u}{\partial x} + \frac{\partial v}{\partial y} + \frac{\partial w}{\partial z} = 0 \qquad (8)$$

in the moving coordinate system by virtue of Eq. 3.

B. Potential Flow Solution for Concentric Spheres in a Moving Coordinate System

The first correct solution for this problem (i.e. the same boundary conditions) was obtained by Stokes (29, 30). The equations will be developed here in order to illustrate this method of determining G(t), and to show the manner in which G(t) enters into the differential equation of motion.

In Fig. 3 the inner sphere of radius a is displaced a distance δ relative to the center 0 of the outer spherical boundary of radius b.

The moving coordinate system is attached to the outer shell or spherical envelope with its center at 0. The moving coordinate system has an absolute velocity of u_o in the x-direction, and the inner sphere has an absolute velocity of V_b in the x-direction. Under these conditions, the velocities are related by

$$V_b = u_o + \dot{\delta} \quad ,$$

and the boundary conditions for the relative velocities are given by

$$r = b \qquad v_r = 0$$

$$r = a \qquad v_r = \dot{\delta} \cos \theta \tag{9}$$

where v_r is the relative radial velocity.

When the amplitude of motion of the inner sphere, δ, is large the second boundary condition given by Eq. 9 is violated in that the true boundary is given by

$$r = \delta \cos \theta + a \left[1 - \left(\frac{\delta}{a} \right)^2 \sin^2 \theta \right]^{\frac{1}{2}}$$

rather than the constant value of a. This effect is neglected in the solution of this problem, and limits the validity of the resulting equations to small amplitudes of motion.

1. <u>Continuity, Laplace, and Euler equations in spherical coordinates</u>

Figure 4 shows the three orthogonal velocity components in a spherical coordinate system (for r, θ, α orientation, see Fig. 2) with respect to the x, y, z coordinate system. Since this problem is axisymmetric with respect to the x-axis, v_α is everywhere zero. Then, the spherical coordinate continuity relationship is

$$\frac{1}{r^2} \frac{\partial}{\partial r} (r^2 v_r) + \frac{1}{r \sin\theta} \frac{\partial}{\partial \theta} (\sin\theta \, v_\theta) = 0 \quad (10)$$

from Eskinazi (9).

The standard procedure for potential flow analysis is to define a potential function ϕ, such that

$$v_r = \frac{\partial \phi}{\partial r}$$

$$v_\theta = \frac{1}{r} \frac{\partial \phi}{\partial \theta} \quad (11)$$

Substitution of Eqs. 11 into Eq. 10 gives

$$\nabla^2 \phi = \frac{1}{r^2} \frac{\partial}{\partial r} \left(r^2 \frac{\partial \phi}{\partial r}\right) + \frac{1}{r^2 \sin\theta} \frac{\partial}{\partial \theta} \left(\sin\theta \frac{\partial \phi}{\partial \theta}\right) = 0 \quad (12)$$

which is the Laplace equation in spherical coordinates for any problem with axisymmetric fluid motion.

Pipes (22) demonstrates that a solution of Eq. 12 may be obtained by using the separation of variables technique. This method of attack gives the solution

$$\phi = \sum_n \left[A_n r^n + B_n r^{(n+1)} \right] P_n(t) \quad (13)$$

where A_n and B_n are arbitrary constants to be determined by the boundary conditions, $P_n(t)$ is the Legendre polynomial of degree n, $t = \cos\theta$, and

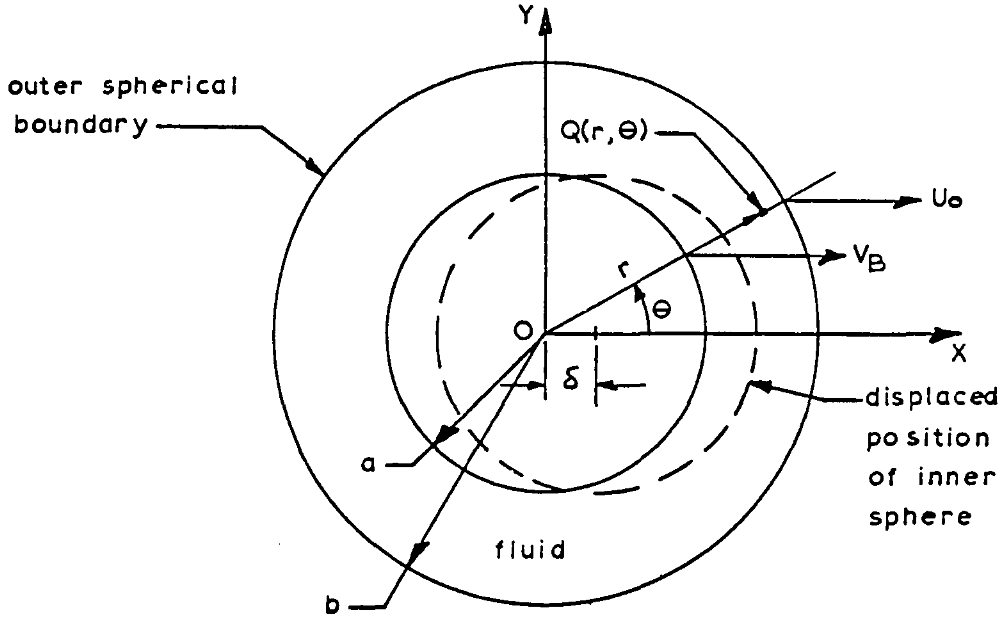

Fig. 3 Geometry of concentric spheres

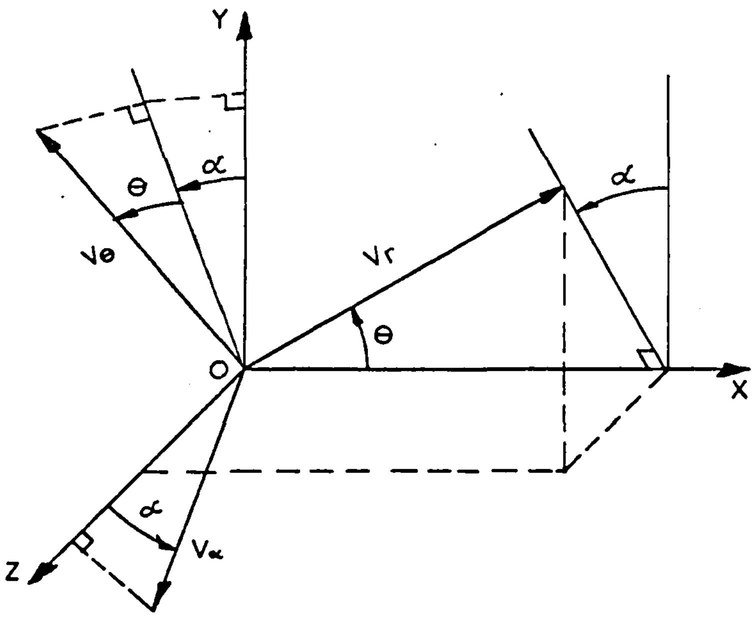

Fig. 4 Spherical coordinate velocity components

the summation ($\sum_n$) is from zero to infinity on the index n.

Pipes (22) shows that the Legendre polynomial is an orthogonal function which may be used to expand an arbitrary function into an infinite series if this function is sectionally continuous in the interval (-1, 1) and the first derivative of the function is continuous on every interior interval.

The radial component of the relative velocity is obtained by combining Eqs. 11 and 13. This gives

$$v_r = \sum_n \left[n A_n r^{(n-1)} - (n+1) B_n r^{-(n+2)} \right] P_n(t) \tag{14}$$

By applying the first boundary condition of Eq. 9, Eq. 14 reduces to

$$(n + 1) B_n = n b^{(2n + 1)} A_n \tag{15}$$

Substitution of Eq. 15 into Eq. 14 gives

$$v_r = \sum_n n A_n \left[\frac{r^{(2n+1)} - b^{(2n+1)}}{r^{(n + 2)}} \right] P_n (t) \tag{16}$$

The secondary boundary condition of Eq. 9 is written in a more convenient form when the cosine is replaced by the equivalent Legendre polynomial, $P_1(t)$. Substitution of the second boundary condition into Eq. 16 gives

$$\dot{\delta} P_1(t) = \sum_n n A_n \left[\frac{a^{(2n + 1)} - b^{(2n + 1)}}{a^{(n + 2)}} \right] P_n(t).$$

Due to the orthogonality properties of Legendre polynomials, it follows that

1. A_o = an arbitrary constant
2. $A_1 = -\dfrac{\dot{\delta}\ a^3}{b^3-a^3}$
3. $A_n = 0$ for $n > 1$.

Then ϕ, v_r, and v_θ are given by

$$\phi = A_o - \left(\frac{\dot{\delta}\ a^3}{b^3-a^3}\right)\left(r + \frac{b^3}{2r^2}\right) \cos\theta = A_o - Dr(1 + \frac{f}{2})\cos\theta, \quad (17)$$

$$v_r = \left(\frac{\dot{\delta}\ a^3}{b^3-a^3}\right)\left(\frac{b^3-r^3}{r^3}\right) \cos\theta = D(f-1)\cos\theta, \quad (16\text{-b})$$

and

$$v_\theta = \left(\frac{\dot{\delta}\ a^3}{b^3-a^3}\right)(1 + \frac{b^3}{2r^3}) \sin\theta = D(1 + \frac{f}{2}) \sin\theta \quad (18)$$

where

$$D = \frac{\dot{\delta}\ a^3}{b^3-a^3}$$

and

$$f = \frac{b^3}{r^3} .$$

Once the relative velocity distribution of the fluid is known in terms of the geometry of the system and velocity of the inner sphere relative to the moving coordinate system, it is possible to determine the pressure distribution on the surface of the inner sphere by using the Euler euqations of motion for an ideal fluid.

For the axisymmetric case in spherical coordinates with a moving coordinate system, the Euler equations may be written as

$$\rho\left(\frac{\partial v_r}{\partial t} + v_r \frac{\partial v_r}{\partial r} + \frac{v_\theta}{r}\frac{\partial v_r}{\partial \theta} - \frac{v_\theta{}^2}{r}\right) = (B_r - \rho a_{ro}) - \frac{\partial P}{\partial r}$$

in the radial direction and

$$\rho\left(\frac{\partial v_\theta}{\partial t} + v_r \frac{\partial v_\theta}{\partial r} + \frac{v_\theta}{r}\frac{\partial v_\theta}{\partial \theta} + \frac{v_r v_\theta}{r}\right) = (B_\theta - \rho a_{\theta o}) - \frac{1}{r}\frac{\partial P}{\partial \theta} \quad (19)$$

in the tangential direction. a_{ro} and $a_{\theta o}$ are the radial and tangential components of the absolute acceleration of the origin of the moving coordinate system. In this problem these components are expressed as

$$a_{ro} = \frac{du_o}{dt} \cos \theta$$

and

$$a_{\theta o} = - \frac{du_o}{dt} \sin \theta \quad (20)$$

The body force due to the weight of the fluid acts vertically downward. The orientation of the x-direction relative to the local direction of gravity is arbitrary, and the angle between the two directions can be β. The body force in the x-direction is given by $B_x = \rho g \cos \beta$, and the body forces in the radial and tangential directions (B_r and B_θ) are given by

$$B_r = \rho g \cos (\theta + \beta)$$

and

$$B_\theta = -\rho g \sin(\theta + \beta)$$

which reduce to

$$B_r = -\rho g \cos\theta$$

and

$$B_\theta = \rho g \sin\theta \tag{21}$$

for the simple case where β = 180 degrees. (Note that the weight of the inner body was neglected in obtaining Eqs. 1 and 1-a). Substitution of Eqs. 16, 18, 20, and 21 into Eq. 19 give the pressure gradient with respect to θ as

$$\frac{\partial P}{\partial \theta} = \rho r\left[\left\{g + \frac{du_o}{dt} - \frac{\dot{D}}{2}(f+2)\right\}\sin\theta + \frac{3}{4}D^2(f^2-4f)\ \frac{\cos\theta\sin\theta}{r}\right] \tag{22}$$

where

$$\dot{D} = \frac{dD}{dt} = \left(\frac{a^3}{b^3-a^3}\right)\ \frac{d\dot{\delta}}{dt}$$

The total change in pressure from point to point in the fluid is given by

$$dP = \frac{\partial P}{\partial r}dr + \frac{\partial P}{\partial \theta}d\theta \quad ,$$

but on the surface of the sphere, dr = 0. Then, if P_1 is the pressure on the surface of the sphere when θ is zero, the pressure at any other point is given by

$$P = P_1 + \int_0^{\theta} \frac{\partial \bar{F}}{\partial \theta}\Big|_{r=a} d\theta \tag{23}$$

Substitution of Eq. 22 into Eq. 23 with the indicated integration gives the pressure at any point on the surface of the sphere as

$$P = P_1 + \rho a\left[\left\{g + \frac{du_o}{dt} - \frac{\dot{D}}{2}(f+2)\right\}(1-\cos\theta) + \frac{3}{8}D^2(f^2-4f)\frac{\sin^2\theta}{r}\right]_{r=a} \tag{24}$$

where f is evaluated for r = a in the bracketed quantity. From Eq. 24, it is possible to determine the force of an ideal fluid on the inner sphere, and consequently the differential equation of motion of the inner sphere relative to the moving coordinate system.

2. Equation of motion of the inner sphere

From Fig. 1-b, it is seen that G(t) is positive to the right. From Figs. 2 and 3, the surface force due to pressure is seen to act in the negative r-direction. The projection of the surface force in the x-direction is negative and is diminished by the cosine of θ, and therefore G(t) is related to the surface force by

$$G(t) = -\int^{A} P\cos\theta\, dA \tag{25}$$

where $dA = 2\pi a^2 \sin\theta\, d\theta$. Substitution of the expression for dA and Eq. 24 into Eq. 25 gives

$$G(t) = 2\pi a^2 \int_0^{\pi}\left[P_1 + \rho a\left\{\left(g + \frac{du_o}{dt} - \frac{\dot{D}}{2}(f+2)\right)(1-\cos\theta)\right.\right.$$

$$+ \frac{3}{8} D^2 (f^2 - 4f) \frac{\sin^2\theta}{r} \Big\} _{r=a} \Bigg] \sin\theta \cos\theta \, d\theta$$

which reduces to

$$G(t) = -M \left[\frac{1}{2} \left(\frac{b^3 + 2a^3}{b^3 - a^3} \right) \frac{d\dot{\delta}}{dt} - (g + \frac{du_o}{dt}) \right] \qquad (25\text{-a})$$

where $M = \frac{4}{3} \pi a^3 \rho$ or the mass of fluid displaced by the sphere.

It is interesting to note that the convective acceleration terms, which are embodied in the $\frac{3}{4} D^2 (f^2 - 4f) \frac{\cos\theta \sin\theta}{r}$ term in Eq. 22, drop out on integration due to cos θ sin θ term. The theoretical significance of this observation with regard to the assumptions made in the viscous flow solution will be discussed in a later section.

The equation of motion for the inner sphere is obtained by substituting Eq. 25-a into Eq. 1-a. The result is

$$\left[m_s + \frac{1}{2} \left(\frac{b^3 + 2a^3}{b^3 - a^3} \right) M \right] \ddot{\delta} + K'\delta = F(t) + Mg + (M - m_s) \frac{du_o}{dt} \qquad (26)$$

where the relationships $m = m_s$, $\delta = x$, and $u_o = \frac{dx_o}{dt}$ were used.

The left-hand side of Eq. 26 is a standard second-order differential equation for a vibrating system without damping. The right-hand side is composed of the forcing functions.

3. Conclusions based on potential solution

Certain observations and conclusions may be drawn from the equations derived in the potential solution. These are:

1. The body force and the "inertia" body force enter into both the Euler and the Navier-Stokes equations in an identical

manner, and if the pressure term due to these terms is factored out of the equations, the body forces will pass through the steps of integration unaltered. Thus, the body force terms may be dropped in carrying out further analysis and these effects may be brought back into the differential equation of motion of any shape of body. This may be expressed mathematically as $G(t) = F + Mg + M \frac{du_o}{dt}$ where F is the resultant fluid force when the body forces are dropped. Note that the signs in the above equation would be reserved if the body forces act in the opposite directions.

2. The convective acceleration terms drop out of the expression for the resultant fluid force, G(t), on the sphere for the potential solution. This is due to the sin θ cos θ product formed in each of the convective terms in Eq. 22 and is independent of the relationship between the velocity components (v_r and v_θ) with respect to the radius r and the time t. This is restricted to a sphere since the change in pressure in the derivation depends only on θ at the surface of the sphere.
3. In order to experimentally determine the effect of the fluid on the inner body, Eq. 26 indicates that the outer boundary or envelope can remain fixed. F(t) can perform the same function as each of the other terms on the right-hand side of Eq. 26 as far as providing a forcing function is concerned.
4. Equation 26 indicates that the mass of the sphere is altered by an additional mass which is concentrated at the geometric center

of the sphere. This added mass is dependent on the geometry of the bodies and the density of the fluid.

5. Equation 26 indicates that "fluid coupling" takes place between the two spheres when the outer envelope or shell is accelerated. This is true regardless of the shape of the envelope and inner body; that is, $M \frac{du_o}{dt}$ is independent of the shapes and is dependent only on the volume of the inner body and the density of the fluid.
6. Since Eq. 26 is a second-order differential equation, the response of the inner sphere should be of the form $e^{j\omega t}$ when the forcing functions are also of this form.
7. A Fourier analysis may be used in this type of problem since all of the terms which remain in the equation of motion of the inner sphere combine linearly. This is a consequence of conclusion 2 above.

C. The Viscous Flow Solution

Stokes (31, 32) presented a paper "On the Effect of Internal Friction of Fluids on the Motion of Pendulums" in 1850. In this paper, he solved the problems of flow about spheres and cylinders in a real fluid and developed what is known today as "Stokes' Stream Function for Axial Symmetry in Three-Dimensional Flow". The development of these stream function relationships is also given in Milne-Thomson (20) and Streeter (33).

The basic assumptions and final equation developed by Stokes will be outlined in the following section. The entire derivation by Stokes is outlined in Appendix A. The nomenclature is that of Stokes except for the following substitutions: j for $\sqrt{-1}$, ω for n, v_r for R, v_θ for θ, ν for μ, and δ for ξ. The starred equation numbers correspond to those of Stokes' for easy reference. Lamb (16) derives the same final equations as Stokes for a sphere in an infinite fluid by using a different approach.

Before solving the problem of two concentric spheres, Stokes considers the following problem which demonstrates the effects of a viscous fluid on a rigid body. Consider an infinitely long plane (or thin plate) which is in an unlimited mass of fluid. The plane is allowed to oscillate in a direction parallel to the plane with a velocity of

$$v = c \sin \omega t \tag{9*}$$

The solution of the governing equations of motion gives a velocity distribution of

$$v = c\, e^{-\sqrt{\frac{\omega}{2\nu}}\, x} \sin \left(\omega t - \sqrt{\frac{\omega}{2\nu}}\, x\right) \tag{12*}$$

above the plane and a force per unit area of

$$T_3 = \rho \sqrt{\frac{\omega}{2\nu}} \left(v + \frac{1}{\omega} \frac{dv}{dt}\right) \tag{13*}$$

which acts on and parallel to the plane. In regard to Eq. 13*, Stokes says, "The force expressed by the first of these terms tends to diminish the amplitude of the oscillations of the plane. The force expressed by the second has the same effect as increasing the inertia of the plane." The significance of this last term cannot be underestimated since it shows that the inertia of a body can be increased by the presence of a real fluid. This term is in excess of the value which may exist from potential flow solutions and may be considered as a thin layer of fluid being carried along by the plane.

The two basic assumptions of Stokes in obtaining the viscous flow solution for two concentric spheres were:

1. The fluid is incompressible.
2. The viscous forces dominate the inertia forces due to the convective acceleration terms, and these acceleration terms are neglected.

The time dependent inertia term must be included since the motion is unsteady. The second assumption is common to viscous or slow flow analysis where the non-linear terms do not drop out due to the boundary conditions and is supported (only for spherical boundaries) by the second conclusion from the previous potential flow analysis.

1. <u>Force of the viscous fluid on the inner sphere and the equation of motion</u>

The resultant fluid force, F, acting on the sphere due to the pressure and shearing stresses of the fluid is given by

$$F = \pi \rho a \frac{d}{dt} \int_0^{\pi} \left\{ a \left(\frac{d\psi_1}{dr} \right)_a + 2 \left(\psi_2 \right)_a \right\} \sin\theta \, d\theta \qquad (49*)$$

from Appendix A. (Note that the body force and "inertia" body force terms are not included in the expression for F. See conclusion 1 of potential flow analysis and the Appendix A for details.) When the stream functions ψ_1 and ψ_2 are substituted and the indicated operations of integration and differentiation are completed, Eq. 49* is reduced to

$$F = \frac{4}{3}\pi\rho a j\omega \left\{ a f_1'(a) + 2 f_2(a) \right\} e^{j\omega t} \qquad (50*)$$

For the case of two concentric spheres, Stokes substituted the relationship

$$K a^2 c = (-k + jC_s) a^2 c = a f_1'(a) + 2 f_2(a)$$

into Eq. 50* where K (= $-k + jC_s$) is a complex function. By noting the definitions of velocity and acceleration, F reduces to

$$F = -(kM)\frac{d\dot{\delta}}{dt} - (M\omega C_s)\dot{\delta} \qquad (27)$$

where M is the mass of fluid displaced by the sphere. Recall that the relationship between G(t) and F is $G(t) = F + Mg + M\frac{du_o}{dt}$ from conclusion 1 of the potential flow analysis. When this form of G(t) is substituted into Eq. 1-a, the differential equation of motion for the inner sphere is

$$(m_s + kM)\ddot{\delta} + (MC_s\omega)\dot{\delta} + K'\delta = F(t) + Mg + (M - m_s)\frac{du_o}{dt} \qquad (26\text{-a})$$

where k is the <u>added mass coefficient</u> and C_s is the <u>fluid damping coefficient</u>. The name of <u>fluid damping coefficient</u> is used here to distinguish

C_s from C'_s where C'_s is the damping coefficient in the usual sense which implies the product of $M \omega C_s$. The term kM shows that the inertia or mass of the sphere is increased, but its weight remains unchanged.

2. Evaluating Stokes' solution

The complex function K was evaluated by applying the boundary conditions of Eqs. 35* and 36* (see appendix A) and by solving the resulting set of four simultaneous equations for the constants A, B, C, and D. The result is

$$K = 1 - \frac{3}{2m^2a^2}\left[\frac{A' - B'}{12ma + C' + D'}\right] \tag{28}$$

where

$$A' = (m^2a^2 + 3ma + 3)(m^2b^2 - 3mb + 3)\ e^{m(b-a)} ,$$

$$B' = (m^2a^2 - 3ma + 3)(m^2b^2 + 3mb + 3)\ e^{-m(b-a)},$$

$$C' = \left[(m^2b^2 - 3mb + 3) - \lambda\ (m^2a^2 + 3ma + 3)\right]\ e^{m(b-a)},$$

$$D' = \left[\lambda(m^2a^2 - 3ma + 3) - (m^2b^2 + 3mb + 3)\right] e^{-m(b-a)} , \tag{29}$$

and

$$\lambda = a/b .$$

Equations 28 and 29 do not reduce easily, but they can be approximated to a satisfactory degree under two conditions.

For the first condition, consider the case when b becomes very large compared to a. Therefore, due to the exponential term

$e^{m(b-a)}$, the quantities given by A' and C' are very large compared to B', D', and 12ma. Under this condition, Eq. 28 reduces to

$$K = -k + j\,C_s = 1 - \frac{3}{2m^2a^2}\left(\frac{A'}{C'}\right), \tag{28-a}$$

and the exponential terms cancel out of A' and C'. This form of K is much easier to work with than the previous one.

For the second condition, consider the case when b is not much larger than a. Upon examination of the similarity of A' and B', it is seen that the major difference between them is the exponential term. The same can be said for C' and D'. Hence, when A' is much larger than B' and C' is much larger than D', the degree of approximation may be estimated by comparing the magnitudes of C' and 12ma.

The calculation of Stokes' solution requires the reduction of A' and C' to their real and imaginary parts. This reduction is simplified when all of the terms are expressed by the two variables β^2 and λ where β^2 $\left(= \frac{\omega a^2}{\nu} = S_n\right)$ is the Stokes' number and λ (= a/b) is the radius or diameter ratio. Through the use of these two variables and Eq. 32*, (see Appendix A) the various terms in A' and C' may be expressed as follows:

$m^2a^2 = j\beta^2$, ma $= \frac{\beta}{\sqrt{2}}(1 + j)$, $m^2b^2 = \frac{\beta^2}{\lambda^2}$, mb $= \frac{\beta}{\lambda}\left(\frac{1 + j}{\sqrt{2}}\right)$,

and $m(b-a) = \frac{\beta}{\sqrt{2}}\left(\frac{1 - \lambda}{\lambda}\right)(1 + j) = h(1 + j)$.

A' may be written in the form of its real and imaginary parts as A' = $(r_1 + jr_2)\ e^{(1+j)h}$ where substitution of the above relationships gives

$$r_1 = 9 - 3h\ (\beta^2/\lambda\ + 3) - (\beta^2/\lambda)^2 \tag{30-a}$$

and

$$r_2 = 3h\ (\beta^2/\lambda\ - 3) + 3\left(\frac{\lambda^2 - 2\lambda + 1}{\lambda}\right) \tag{30-b}$$

In a like manner, C' may be written as $C' = (r_5 + jr_6)e^{(1+j)h}$ where the substitution gives

$$r_5 = 3(1 - \lambda) - \left(\frac{1 + \lambda^2}{1 - \lambda}\right)\ (3h) \tag{30-c}$$

and

$$r_6 = \left(\frac{1 - \lambda^3}{\lambda}\right)\ (\beta^2/\lambda) - 3h\left(\frac{1 + \lambda^2}{1 - \lambda}\right) \tag{30-d}$$

Substitution of Eqs. 30-a through 30-d into Eq. 28-a and cancellation of the common $e^{(1+j)h}$ factor give the reduction of K to its real and imaginary parts as

$$k = \frac{3(r_2 r_5 - r_1 r_6)}{2\beta^2\ (r_5^2 + r_6^2)} - 1 \tag{30-e}$$

and

$$C_s = \frac{3\ (r_1 r_5 + r_2 r_6)}{2\beta^2\ (r_5^2 + r_6^2)}\quad . \tag{30-f}$$

These are close approximations for k and C_s when the values of β^2 are greater than 10^3 for $\lambda = 0.74$. It can be shown that the difference between C' and 12 ma is about one percent when β^2 is equal to 400. Since the lowest value of β^2 in the experimental work was approximately 400, Stokes' solution was calculated from Eqs. 30-a through 30-f.

3. Summary of the theoretical analysis

As noted previously, an experimental program can be set up with the outer shell fixed since the dynamic response characteristics of the equation of motion depends on the left-hand side of Eq. 26-a for a given forcing function. Equations 30-a through 30-f of the viscous flow solution indicate that k and C_s depend on the values of Stokes' number (S_n) and the radius ratio λ while the potential flow solution indicates C_s is zero and k depends only on λ.

In summary, the theoretical analysis has shown that:

1. The equation of motion is a second-order differential equation.
2. The coefficients of the second-order differential equation are not constant but depend on Stokes' number for a given geometry.
3. The mass or inertia of the body is increased by the added mass, kM, which acts through the centroid of the body but does not alter the weight of the body.
4. The body force and "inertia" body force appear as forcing functions in the equation of motion.
5. The outer shell may be fixed for conducting the experimental program since the effects of the viscous fluid on the equation of motion are contained in the terms k and C_s; that is, these are the only terms in equation of motion which are functions of Stokes' number.

The viscous and potential flow solutions are the extremes of analysis since the convective acceleration terms are neglected in the first and the viscous terms are neglected in the second. An experimental program must be utilized to establish the range over which these theoretical methods of approach are valid and must fill the void between these two extremes of analysis where the convective acceleration terms and the viscous terms are of equal importance.

With the potential and viscous flow solutions worked out, a more rational basis for the establishment of the experimental program is available. In this regard, the theoretical analysis will be of assistance in selecting the variables to be considered and the most useful forms for the Pi-terms.

III. DIMENSIONAL ANALYSIS

Dimensional analysis provides a means to systematize and simplify the experimental program. The number of variables in the experimental program are reduced by replacing the original variables with dimensionless Pi terms where each Pi term is a function of one or more of the original variables. The Pi terms provide more experimental freedom since it is usually possible to change the value of a dependent Pi term by varying one or more of the original variables and to hold the remaining dependent Pi terms constant.

The selection of the pertinent variables, of course, is the most difficult part of this analysis since the omission of an important variable can lead to erroneous conclusions. This selection is divided into two groups; i.e., the variables which are included in the previous theoretical work and those which are not.

A. The Selection of Variables and Pi Terms

1. Added mass variables

The added mass is seen from the theoretical analysis to depend on the following variables.

1. ρ - the density of the fluid - FT^2L^{-4}
2. ν - the kinematic viscosity of the fluid - L^2T^{-1}
3. a - the radius of the inner sphere - L
4. b - the radius of the outer sphere - L
5. ω - the angular frequency of the oscillation - T^{-1}

where F, L, and T stand for force, length, and time, respectively. The variables not included in the theoretical analysis are

6. $\overline{\delta}$ - the amplitude of the oscillation - L

7. ϵ - the mean height of the surface protrusions or roughness of the surface - L

8. E - the rigidity parameter of the spherical boundary - FL^{-3}

It can be shown that the outer shell is subjected to a fluctuating pressure. The resulting elastic deformation is a vibration of the shell which violates the boundary conditions as stated in the viscous flow solution. Thus, the rigidity of the shell must be considered if the shell vibration is to be avoided and the boundary conditions are to be satisfied. The rigidity parameter is a function of the properties of the material, the geometrical configuration of the material, and the external loads applied to the shell. The inclusion of these additional variables is beyond the scope of this study. The rigidity parameter was introduced to represent these elastic effects by a single term which is considered to a measure of the rigidity of the outer shell. The dimensions of FL^{-3} were given to the rigidity parameter since the resulting Pi term will include an important combination of variables and have a simple but useful form.

In the original dimensional analysis, the rigidity parameter was omitted. The exclusion of this variable led to the designing of the basic experimental procedure on an erroneous basis which, in turn, gave some experimental scatter. The added mass (M' - FT^2L^{-1}) may be expressed in a general equation as

$$M' = f(\rho, \nu, a, b, \omega, \bar{\delta}, \epsilon, E) \qquad (31\text{-a})$$

with a total of eight independent variables and one dependent variable.

2. Damping coefficient variables

The damping coefficient (C'_s - FTL^{-1}) is a function of the same variables as the added mass with the possible exception of the rigidity parameter of the spherical boundaries. However, for completeness, it is included here as a variable. The damping coefficient may be expressed in a general form as

$$C'_s = g(\rho, \nu, a, b, \omega, \bar{\delta}, \epsilon, E) \qquad (31\text{-b})$$

with a total of eight independent variables and one dependent variable.

3. Buckingham Pi Theorem

The Buckingham Pi Theorem was used to express Eqs. 31-a and 31-b in terms of dimensionless parameters. Murphy (21) states this theorem as follows: "In general terms, the Buckingham Pi Theorem states that the number of dimensionless and independent quantities required to express a relationship among the variables in any phenomenon is equal to the number of quantities involved, minus the number of dimensions in which those quantities may be measured. In equation form the Pi Theorem is

$$s = n - b,$$

in which s is the number of π terms

n is the total number of quantities involved

b is the number of basic dimensions involved."

Thus, there are nine variables and three basic dimensions in this problem which, according to Buckingham's Pi Theorem, must give six independent and dimensionless terms. The exact form of the Pi terms is arbitrary as long as they are independent and dimensionless. However, it is judicious to develop as many Pi terms as possible which will correspond to the dimensionless terms formed in the viscous flow solution.

4. Pi terms

The six Pi terms considered in the experimental study of the added mass were:

1. $\pi_1' = \frac{M'}{\rho a^3}$ where the a^3 could be replaced by any combination of a^2b, ab^2, etc. Stokes' solution associates M' with the mass of fluid displaced by the sphere. Hence, the first Pi term, which is the dependent term, is written as

$$\pi_1 = \frac{M'}{\frac{4}{3}\rho a^3} = \frac{M'}{M} = k$$

since $\frac{4}{3}\pi$ is a dimensionless constant.

2. $\pi_2 = \frac{\omega a^2}{\nu} = S_n$ where ωa could be replaced by $\omega\bar{\delta}$ which is the maximum velocity. Stokes' solution indicates the combination of $\frac{\omega a^2}{\nu}$. This term is a measure of the ratio of the inertia forces to the viscous forces in the fluid and is considered to be a form of Reynolds number for this problem. The title of Stokes' number is used in honor of Stokes in the literature.

3. $\pi_3 = \frac{a}{b} = \lambda$ where the ratio b/a could also be used. Since b can become large or infinite, it is more convenient to use the

ratio of a/b which gives λ values between zero and one.

4. $\pi_4 = \frac{\bar{\delta}}{a}$ where $\bar{\delta}/a$ is used in place of $\bar{\delta}/b$ or $\bar{\delta}/\epsilon$. As shown in the potential flow analysis, the ratio of δ/a is a measure of the errors associated with the assumption that $r = a$ describes the inner boundary at all times.

5. $\pi_5 = \frac{\epsilon}{a}$ which is a measure of the relative roughness of the inner sphere.

6. $\pi_6 = \frac{\rho\omega^2\bar{\delta}}{E}$ From Eq. 24, it is possible to show that the fluctuating pressure which acts on the outer boundary is proportional to $\rho\omega^2\bar{\delta}$.

If the outer boundary were quite flexible, this would alter the outer boundary condition from a radial velocity of zero to some finite value which may not be in phase with the pressure. The radial velocity component induced by the fluctuating pressure term may be increased by a factor of 4 when ρ, $\bar{\delta}$, and the shell are the same and ω is allowed to double. This indicates that the stiffness of of the outer shell is of great importance and π_6 is a measure of this elastic boundary effect. The effect of this phenomenon was detected in the experimental data to be discussed later. The dimensionless equation for the added mass can be written in the form

$$\pi_1 = k = F(\pi_2, \pi_3, \pi_4, \pi_5, \pi_6) \tag{32-a}$$

where

$$\pi_1 = \frac{M'}{M} = k, \ \pi_2 = \frac{\omega a^2}{\nu} = S_n, \ \pi_3 = \frac{a}{b} = \lambda \ , \ \pi_4 = \bar{\delta}/a,$$

$$\pi_5 = \frac{\epsilon}{a} \ , \ \pi_6 = \frac{\rho\,\omega^2\bar{\delta}}{E} \quad \text{, and F is an unknown function .}$$

For the damping coefficient, the Pi terms are the same except for the dependent Pi term which contains the dependent variable C_s'. The lead given by the viscous solution indicates this Pi term should be written as

$$\pi_7 = \frac{C_s'}{\frac{4}{3}\pi\rho a^3} = \frac{C_s'}{M} = C_s$$

Then, the dimensionless equation for the fluid damping coefficient can be written in the general form of

$$\pi_7 = C_s = G(\pi_2, \pi_3, \pi_4, \pi_5, \pi_6) \qquad (32\text{-b})$$

where π_2, π_3, etc. are the same as before. From Eqs. 32-a and 32-b, it is possible to examine some of the requirements for an experimental program.

B. Control of Pi Terms

The object of the experiments was to determine π_1 and π_7 as functions of π_2 for a given π_3. As can be seen from Eqs. 32-a and 32-b, the experimental objective requires that the Pi term π_4, π_5, and π_6 be held constant. In regard to π_5, this could be readily accomplished, but the terms π_2, π_4, and π_6 presented a more difficult problem.

In order to obtain the widest possible range for π_2 three possibilities were available:

1. Vary a. This requires constructing many inner and outer spheres to hold π_3 constant, and is a rather poor choice because π_4, π_5,

and π_6 are affected.

2. Vary ω. This is easily done but gives rise to the problem of holding π_4 and π_6 constant since one or the other must change.

3. Vary ν. This is a laborious job with the problem of fluids mixing and changing properties. The changing of fluids will most likely change the density and, hence, change π_6.

These three alternatives show that π_2, π_4, and π_6 are somewhat incompatible because of a change in π_2, with ω, a, or ν, will also change π_4 and/or π_6.

The final experimental procedure was based on two assumptions:

1. The results will not be seriously effected as long as the center of the inner sphere remains within a small volume at the center of the outer sphere. This implies that π_1 and π_7 are nearly independent of π_4 for small values of π_4. This will allow some freedom and is supported by experimental observation.

2. The spheres (inner and outer) are rigid, and the elastic behavior may be neglected for a moderate range of frequencies. Then, π_6 may be considered to have a negligible effect on the results.

If these two assumptions are accepted, it is possible to hold π_3 and π_5 constant with some variation in π_4 and π_6. π_2 could be made to cover the range of 4×10^2 to 6×10^5 by using four different fluids and by varying ω from approximately 5 cycles per second to 25 cycles per second, and π_6 was increased by a factor of about 25 with ρ and $\bar{\delta}$ held constant. Thus, assumption two which was made without the benefit of π_6 originally may be expected to give some trouble when ω is at its higher values. This was verified experimentally.

IV. EXPERIMENTAL PROCEDURE AND APPARATUS

A. Development of the Experimental Procedure

From Eq. 26-a, it is seen that the governing differential equation for the sphere is a second-order equation with varying coefficients since k and C_s are expected to be functions of $\frac{\omega a^2}{\nu}$ from the viscous flow solution. For a given sphere and fluid, the coefficients depend entirely on the angular frequency. When ω is constant, the coefficients are also constant. Thus it appears reasonable to conclude that the solution and response of this equation is very similar to the solution and response of a second-order differential equation with constant coefficients. Hence, it was assumed that the equation governing the vibration of the sphere could be treated as an ordinary second-order differential equation with constant coefficients when the angular frequency was constant.

On the supposition that this assumption is valid, a vibratory system as shown in Fig. 5-a was proposed in which the inner sphere is attached to a simply supported beam with a spring constant of K_b. The beam and sphere were driven by a spring attached to the loud-speaker probe. The driving spring has a spring constant of K_s, and the speaker probe moves with a motion of h cos ωt. From the theory of vibrations, it can be shown that the first mode of vibration of a simply supported beam is the same as a weightless beam with approximately half the mass of the beam concentrated at the center. Since the sphere and the spring were attached to the center of the beam by a device having mass, all mass,

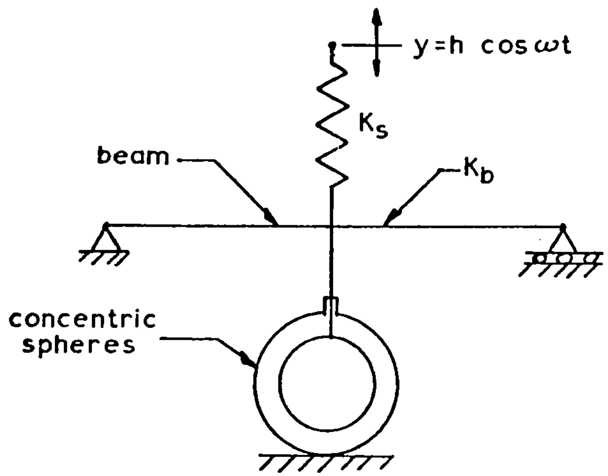

Fig. 5-a Beam with attached sphere

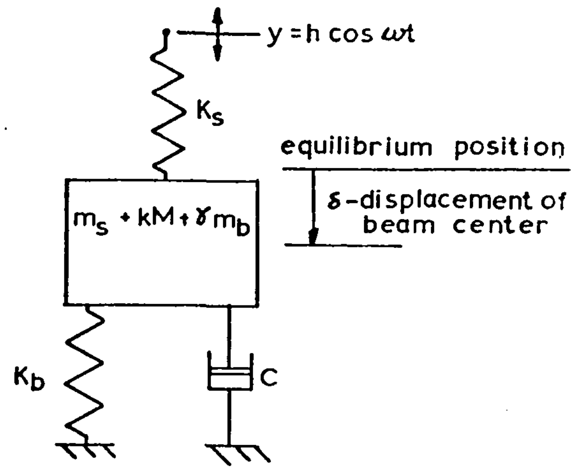

Fig. 5-b Equivalent spring, mass, and dashpot system

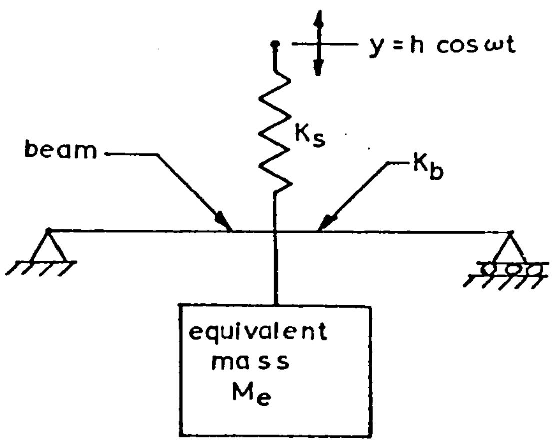

Fig. 6-a Beam with equivalent mass attached

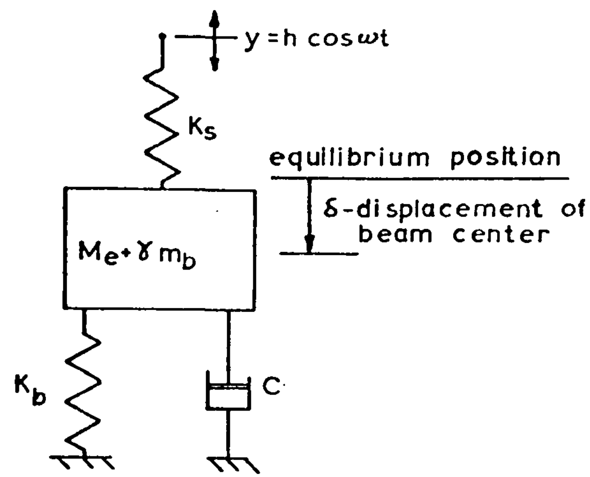

Fig. 6-b Equivalent spring, mass, and dashpot system

other than that of the sphere and added mass, was combined in a term proportional to the mass of the beam and written as γm_b.

An equivalent system is shown in Fig. 5-b in the form of a simple spring, mass, and dash-pot. The equation of motion can be obtained from Eq. 26-a by setting

$$F(t) = K_s \, h \cos \omega t - \gamma m_b \ddot{\delta} - C_b' \dot{\delta}$$

$$K' = K_b + K_s$$

and all other terms on the right hand side equal to zero. Newton's second law may be applied to a free body diagram of the body in Fig. 5-b to also obtain the equation of motion. Both methods give

$$(m_s + kM + \gamma m_b) \ddot{\delta} + C \dot{\delta} + (K_b + K_s) \delta = K_s \, h \cos \omega t \qquad (33)$$

where the weights and bouyant forces are neglected since they give a particular solution of δ equal to a constant. The damping coefficient C is the sum of the damping coefficients for the beam and the sphere.

The beam shown in Fig. 6-a has a mass of M_e attached at its center. If Newton's second law is applied to a free body diagram of the body in Fig. 6-b, the equation of motion is

$$(M_e + \gamma m_b) \ddot{\delta} + C' \dot{\delta} + (K_b + K_s) \delta = K_s \, h \cos \omega t. \qquad (34)$$

If it is assumed that the two beams and their respective spring constants are the same, that the term γm_b and the frequency of the forcing function are the same, and that the two systems are in resonance with the same natural frequency, then it follows that $M_e = m_s + kM$. From this equation, the added mass coefficient is given by

$$k = \frac{M_e - m_s}{M} \tag{35}$$

The most direct method for determining the damping coefficient of a vibrating system is to measure the logarithmic decrement of damped vibration curves, and this technique was used to evaluate the damping.

An alternate method for determining the added mass coefficient is given by Sarpkaya (26). His method consists of using a load cell between the vibrating beam and the sphere which measures the external force on the sphere. This method was considered to be unacceptable since the equipment needed careful calibration for each run and the isolation of the damping and mass terms would have been extremely difficult.

The preceding paragraphs have shown that the desired information can be obtained from a vibrating beam with a sphere and an equivalent mass attached. The fundamental information and the necessary equations which are needed for the experimental program are presented as five separate procedures which formed the basis for the final experimental procedure. From these five procedures, the added mass and the fluid damping coefficients were determined.

PROCEDURE I The sphere is attached to the beam and the driving frequency adjusted until resonance occurs. (At this point, it is assumed that the natural frequency can be accurately determined.) The power to the speaker is cut off, and a damped vibration trace is recorded. From Eq. 33 with h set equal to zero, the differential equation of motion is

$$m_1 \ddot{\delta} + C_1 \dot{\delta} + K_1 \delta = 0 \qquad (33\text{-a})$$

where $m_1 = m_s + kM + \gamma_1 m_b$.

From vibration theory, the damping coefficient is given by

$$C_1 = C_s' + C_{b1} = \left(\frac{m_1 \omega_1}{n_1 \pi}\right) \ln \left(\frac{X_1}{X_{n1}}\right)$$

where C_s' is the damping coefficient of the sphere, C_{b1} is the damping coefficient of the beam, X_1 and X_{n1} are the amplitudes of the damped curve at the beginning and at the nl th cycle, ω_1 is the damped frequency, and nl is the number of cycles over which the logarithmic decrement is measured. From the damped trace, ω_1, X_1, and X_{n1} can be obtained. Hence, this procedure gives the damping coefficient of the sphere and beam combination and the damped frequency ω_1.

PROCEDURE II The sphere is attached to the beam, and the system is driven at the natural frequency. The differential equation is

$$m_2 \ddot{\delta} + C_2 \dot{\delta} + K_2 \delta = K_s h_2 \cos \omega_2 t \qquad (33\text{-b})$$

from Eq. 33 where $m_2 = m_s + kM + \gamma_2 m_b$. The forcing frequency is given by

$$\omega_2 = \sqrt{\frac{K_2}{m_2}} = \sqrt{\frac{K_1}{m_1}} \qquad (36)$$

and is recorded as the natural frequency of the system.

PROCEDURE III The sphere is replaced by a mass at the center of the beam. The mass is adjusted until the system is vibrating in resonance with the driving frequency set at ω_2. The driving frequency is recorded to check the possiblity of drift. From Eq. 34, the governing equation of motion is

$$m_3\ddot{\delta} + C_3\dot{\delta} + K_3\delta = K_s h_3 \cos \omega_3 t \qquad (34\text{-a})$$

where $m_3 = M_e + \gamma_3 m_b$.

PROCEDURE IV The mass remains the same. The beam is driven by the speaker, and then the power is cut off. A damped vibration trace is recorded. From Eq. 34 with h set equal to zero, the differential equation of motion is

$$m_4\ddot{\delta} + C_4\dot{\delta} + K_4\delta = 0 \qquad (34\text{-b})$$

where $m_4 = M_e + \gamma_4 m_b$. The damping coefficient is

$$C_4 = C_{b4} + C_{m4} = \left(\frac{m_4 \omega_4}{n_4 \pi}\right) \ln \left(\frac{X_4}{X_{n4}}\right)$$

where C_{b4} is the beam damping coefficient, C_{m4} is the damping coefficient due to the presence of the equivalent mass container and ω_4 is the damped frequency.

The assumptions associated with Eq. 35 may be expressed as $K_1 = K_2 = K_3 = K_4$, $\gamma_1 = \gamma_2 = \gamma_3 = \gamma_4$, $\omega_2 = \omega_3$, and $m_1 = m_2 = m_3 = m_4$. The first result of these assumptions is the added mass coefficient given by Eq. 35. The second result is the damping coefficient of the sphere which is obtained by subtracting C_4 from C_1. This subtraction gives $C_1 - C_4 = C'_s + C_{b1} - C_{b4} - C_{m4}$ which can be written as

$$C'_s = C_1 - C_4 + (C_{b4} - C_{b1}) + C_{m4}.$$

The damping coefficient of the sphere reduces to

$$C'_s = C_1 - C_4 \tag{37}$$

if it is assumed that $C_{b1} = C_{b4}$ and that C_{m4} is negligible compared to C'_s. Substitution of the expressions for C_1 and C_4 into Eq. 37 yields

$$C'_s = \frac{m_4}{\pi}\left[\frac{\omega_1}{n_1}\ln\frac{X_1}{X_{n1}} - \frac{\omega_4}{n_4}\ln\frac{X_4}{X_{n4}}\right] \tag{37-a}$$

The principal difficulty with Eq. 37-a is the mass term m_4. From Eq. 36, it can be seen that m, K, and ω are related to each other, but any calibration of the spring constant is considered to be of questionable value unless the calibration is done during each experiment since the beam is changed to vary $\omega a^2/\nu$. This leads to the need for procedure V in which m_4 is determined experimentally during each run of data.

PROCEDURE V A mass m_a which is in excess of M_e is attached to the center of the beam. The frequency is adjusted until resonance occurs, and the driving frequency is recorded. From Eq. 34, the governing equation of motion is

$$m_5\ddot{\delta} + C_5\dot{\delta} + K_5\delta = K_s h_5 \cos \omega_5 t \tag{34-c}$$

where $m_5 = m_a + m_4$, and $K_5 = K_4$.

From the relationships between masses, spring constants, and natural frequencies, it can be shown that

$$m_4 = m_a \left(\frac{\omega_5^2}{\omega_2^2 - \omega_5^2} \right) \tag{38}$$

From Eq. 27, the fluid damping coefficient is related to the damping coefficient by

$$C_s = \frac{C'_s}{M \omega_2} \tag{39}$$

Substitution of Eqs. 37-a and 38 into Eq. 39 gives the fluid damping coefficient as

$$C_s = \frac{1}{\pi} \left(\frac{m_a}{M}\right)\left(\frac{\omega_5^2}{\omega_2^2 - \omega_5^2}\right)\left[\frac{1}{n_1} \ln \frac{X_1}{X_{n1}} - \frac{1}{n_4} \ln \frac{X_4}{X_{n4}}\right] \tag{39-a}$$

if it is assumed that $\omega_1 = \omega_2 = \omega_4$. Hence, it is possible to determine both k and C_s from Eqs. 35 and 39-a with this type of arrangement provided the natural frequency can be accurately determined.

B. Instrumentation Technique

The steady state solution of Eqs. 33 and 34 is of the form

$$\delta = \frac{K_s h}{\sqrt{(K-m\omega^2)^2 + C^2\omega^2}} \cos (\omega t - \alpha) \tag{40-a}$$

where α is the phase angle between δ and the driving force and is given by

$$\tan \alpha = \frac{C\omega}{K - m\omega^2} \quad . \tag{40-b}$$

When ω is the natural frequency, the tangent of α is infinity. This indicates that α is 90 degrees; that is, there is a phase shift of 90 degrees between the forcing function (K_s h cos ωt) and the response of δ which is given by Eq. 40-a. Since a phase shift of 90 degrees always occurs when ω is the same as the natural frequency, a direct measurement of the phase shift may be used to determine if the driving frequency is the same as the natural frequency.

1. Measurement of phase shift

The phase angle can be measured by using Lissajous figures as follows:

Let the horizontal displacement of a point be given by $x = a \cos \omega t$, and the vertical displacement be given by $y = b \cos (\omega t - \alpha)$. Now, consider two cases: $\alpha = 0$ and $\alpha = 90$ degrees. In the first case, the relationship between y and x is $y = \frac{b}{a} x$, and in the second, $\frac{x^2}{a^2} + \frac{y^2}{b^2} = 1$. Hence, the relationship between y and x goes from a straight line to an ellipse which reduces to a circle when $a = b$.

When a displacement pickup which measures the displacement of the speaker probe (h cos ωt) is connected to the horizontal amplifier of an oscilloscope and a similar pickup which measures the displacement of the beam or sphere is connected to the vertical amplifier of the same oscilloscope, an ellipse or circle is traced on the screen when α = 90 degrees. The prime requirement for using this technique is that the relative phase shift between the two displacement measuring instruments and the presentation of their signals on the scope be zero over the frequency range used.

2. Instrumentation and equipment

A schematic diagram of the basic instrumentation is shown in Fig. 7. The oscillator drives the Heathkit amplifier with a sinusoidal voltage. The amplifier drives the speaker probe which drives the beam through the drive spring K_s. Pickup #1 measures the displacement of the speaker probe, and the signals are amplified by the Brush amplifier #1 which is connected to the horizontal amplifier of the scope. Pickup # 2 measures the displacement of the center of the beam, and the signals are amplified by the Brush amplifier #2 which is connected to the vertical amplifier of the scope. A recorder is connected to the Brush amplifier #2 for recording either the steady state or damped oscillation of the beam.

The equipment used is listed as follows:

1. Oscillator - Hewlett Packard (low frequency) Model 202C.
2. Amplifier - Heathkit hi-fi amplifier (25 watts) Model W-5M.
3. Speaker - 12 inch permanent magnet type with probe glued to voice coil and center guided.

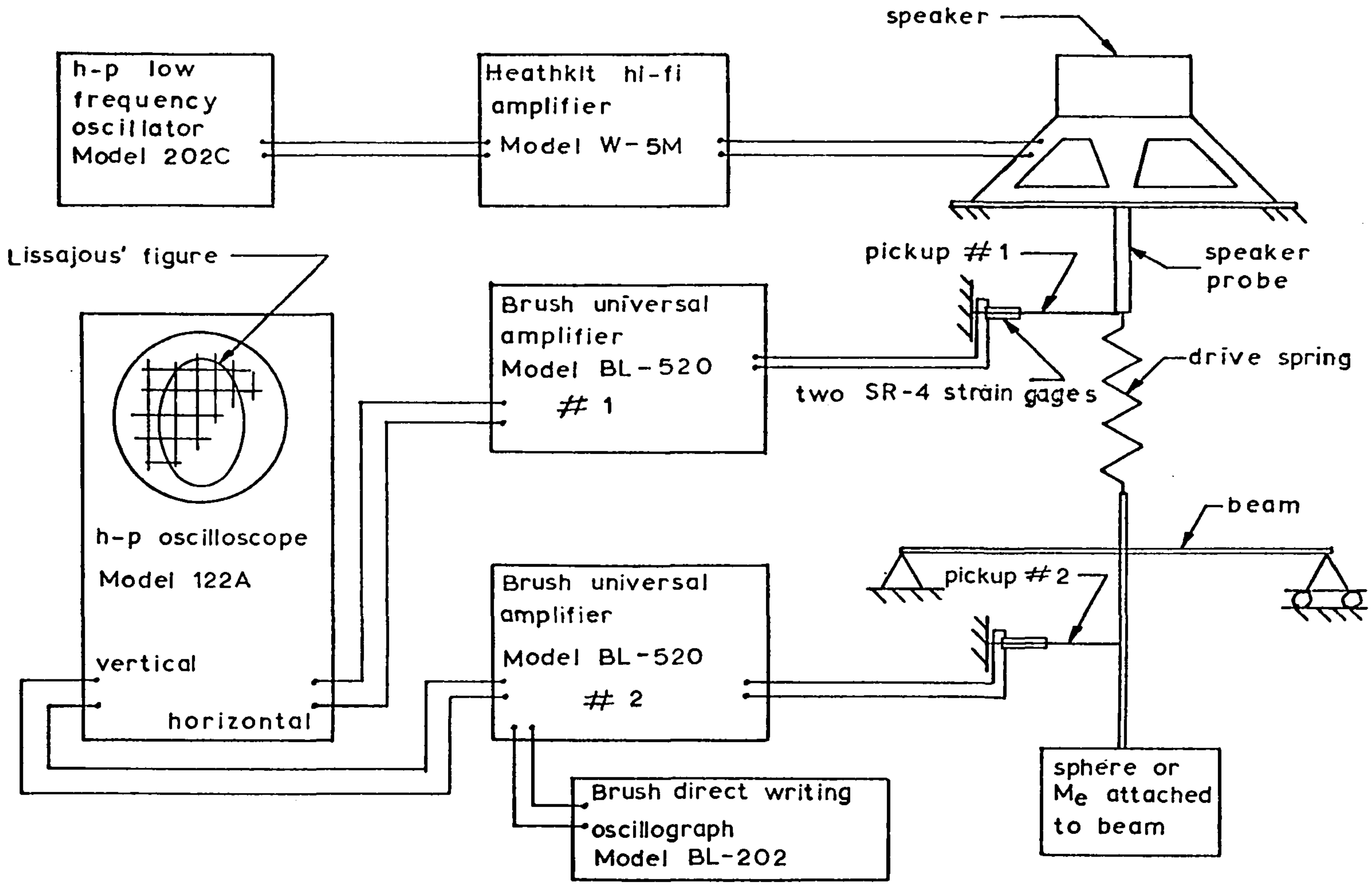

Fig. 7 Schematic diagram of instrumentation

4. Pickup #1 - two SR-4 gages glued to steel scale which was bolted between two 1/4 inch steel plates.
5. Pickup #2 - three types were used and are described in more detail in the next section.
6. Brush universal amplifiers #1 and #2 - these were identical Brush amplifiers - model BL-520.
7. Oscilloscope - Hewlett Packard Model 122A.
8. Recorder - Brush direct writing oscillograph Model BL-202.

3. Beam pickups

Three types of pickups were used to measure the displacement of the beam. The first two types presented some entirely unexpected problems.

TYPE ONE The first pickup was a displacement type, manufactured by Brush (Model DP-1), which used a crystal element to generate an electrical signal. This pickup could be connected directly to the oscilloscope or the Brush amplifier #2 for recording purposes.

It was observed that a phase shift occurred when the position of the pickup was altered slightly relative to the beam with the driving frequency constant. This was undesirable, but it was also observed that the phase shift was sensitive to the input resistance of the oscilloscope. An analysis of the electrical circuit for the pickup showed that the phase shift was dependent on the input resistance and was strongly frequency dependent over the range of frequencies used.

TYPE TWO The second pickup used on the beam was identical to the pickup used on the speaker probe. When both pickups were connected to the speaker probe, they gave identical signals on the scope with no phase shift between them over a frequency range of 4 to 100 cycles per second. This pickup was used for obtaining a large amount of data, but it was found, after several refinements were made in other parts of the apparatus, that a change in the equilibrium position of this pickup by 1/8 of an inch would change the value of M_e by about 5 percent for a constant driving frequency on the lightest beam.

TYPE THREE Two SR-4 gages were glued to the beams about one and one half inches from their centers. One gage was mounted on the top and one on the bottom of each beam. These gages measured strains in the beam which are proportional to the displacement of the centers of the beam.

In order to check on the phase relation between the speaker probe pickup #1 and this pickup, the type two pickup was also attached to the center of the beam. The oscillator was adjusted until the beam was vibrating at resonance. The type two pickup was then connected to the scope through the #1 Brush amplifier, and the two signals (one from the type two pickup and one from the strain gage on the beams) were compared for phase on the scope. No phase shift occurred. To insure that speaker pickup #1 and the type two pickup had no phase shift between them, both were connected to the speaker probe and tested. This test procedure was used before and after the last series of data.

Type three pickup solved the problem of pickup interference into the performance of the lightest beam. Once the oscillator was set at the natural frequency, the mass attached at the center could be removed and replaced, and the beam could be externally disturbed; but, when the disturbance stopped, no changes occurred in the natural frequency.

C. Description of Apparatus

1. Supporting frame

The frame used to support the various parts of the apparatus is shown in Figs. 8 and 9. This frame was built of construction grade 2 in. x 6 in. lumber. The left end was bolted to a brick wall, and the bottom was anchored to the concrete floor. The outer shell was attached to the moving support which could be raised and lowered during the experiment. The speaker, the beam, the fluid reservoir, and the vibration pickups were supported by the top support.

2. Vibrating beams and supports

The vibrating beams which were used as variable springs in the experiment were originally designed to give a frequency range of 4 to 40 cycles per second. It was found, however, that the three lightest beams were too flexible for the mass they had to carry and the four heaviest beams were too stiff for the supporting frame. In the latter case, the supporting frame vibrated more than the beams when resonance was reached.

It became apparent during the preliminary tests that three or four beams would be sufficient. The physical description of the four beams used is given in Table 1.

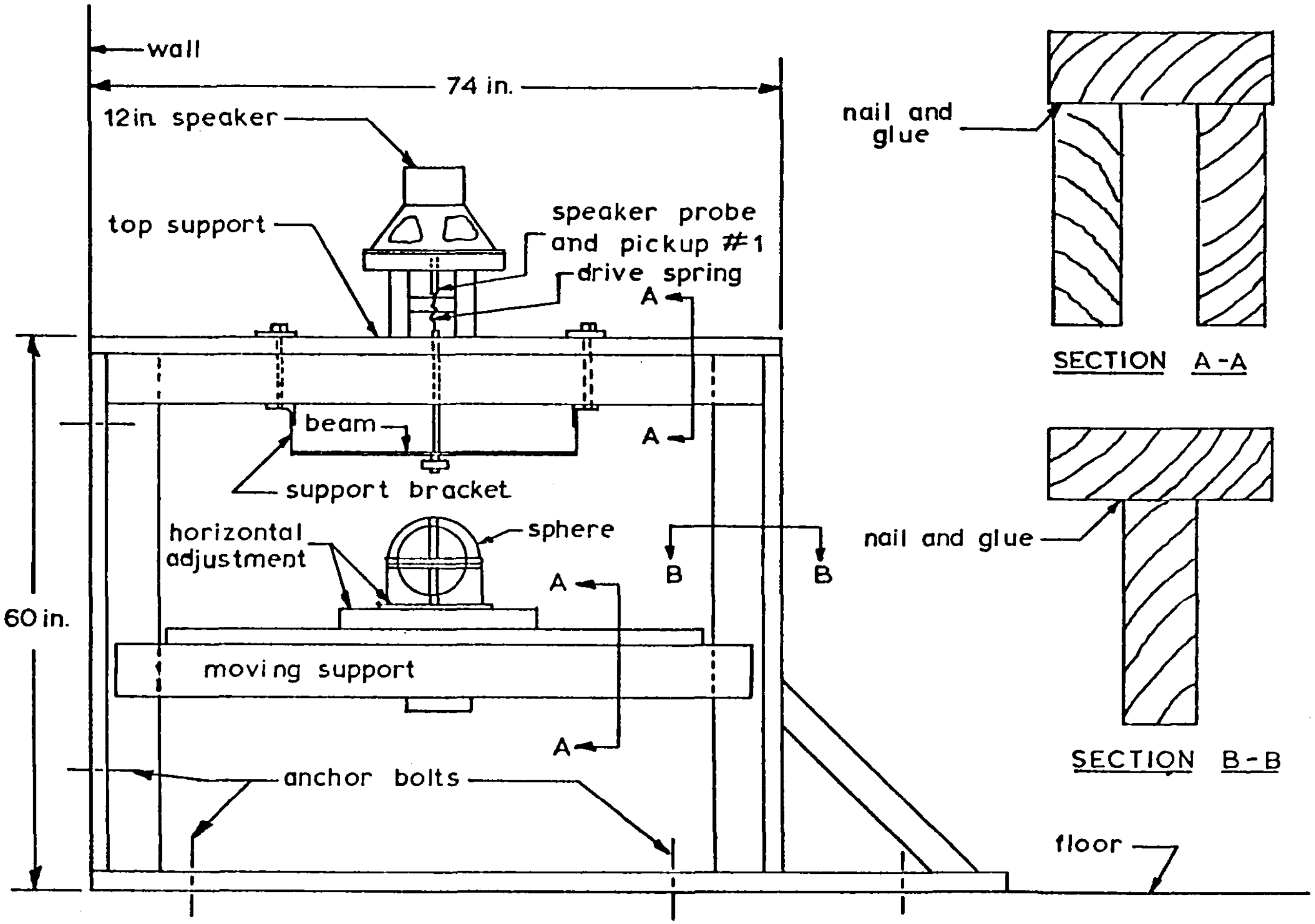

Fig. 8 Supporting frame

Fig. 9 Supporting frame

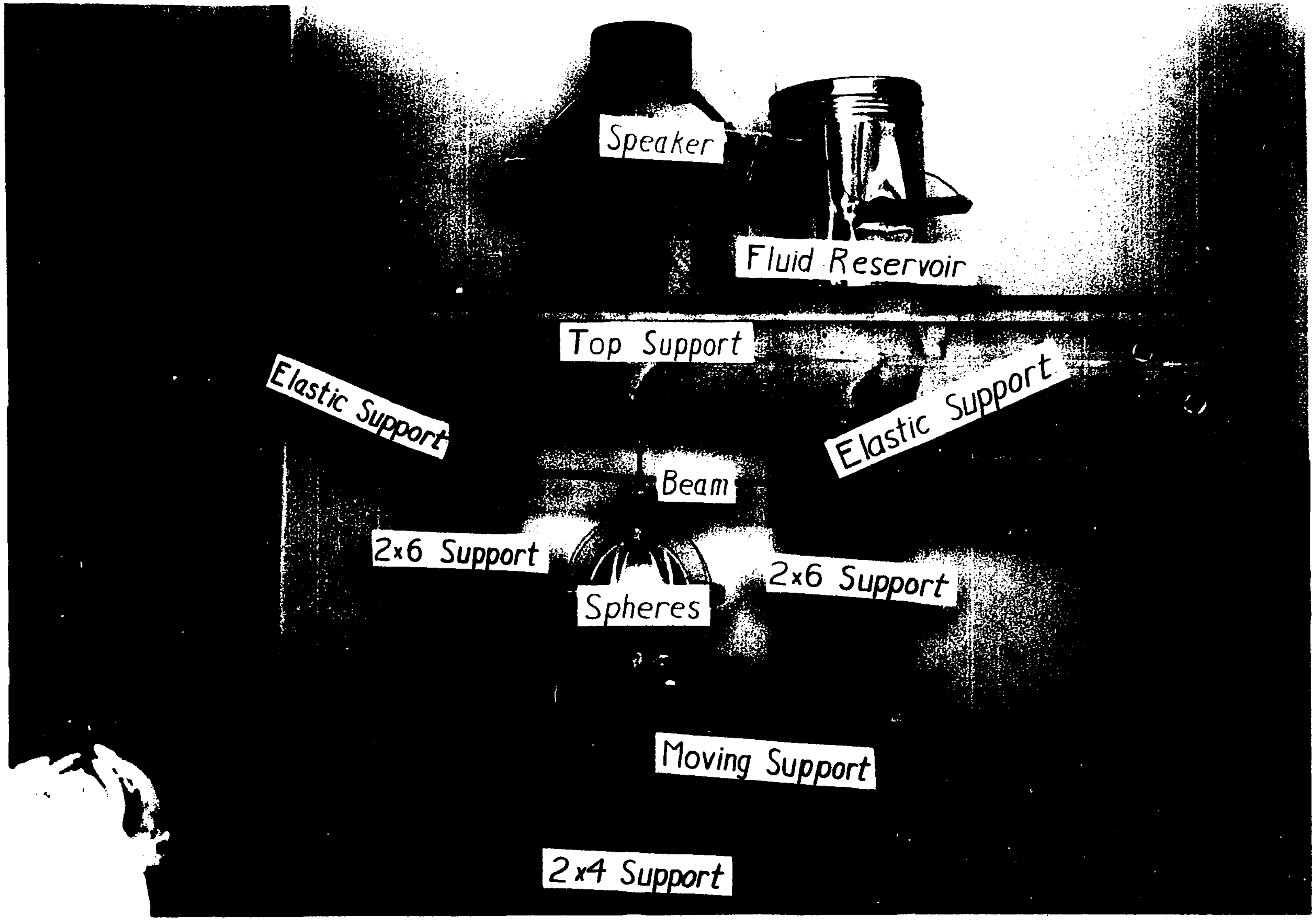
Speaker
Fluid Reservoir
Top Support
Elastic Support
Elastic Support
Beam
2x6 Support
2x6 Support
Spheres
Moving Support
2x4 Support

Table 1. Beam sizes

Beam no.	Material	b(width) in.	h(depth) in.	l(length) in.
4	Aluminum	1	1/4	31.0
7	Steel	1	1/4	34.0
9	Steel	1	1/4	24.5
12	Steel	1	1/2	30.5

These sizes gave a frequency range of about five to twenty-three cycles per second.

a. Linearity of beams Beam numbers 4 and 7 deflected considerably under the load of the equivalent mass which they had to carry, and there was some concern as to whether or not the beams were operating at a point where the spring constant was non-linear. A static test was conducted to determine if the load-deflection diagram showed any non-linearities. The results of this test indicated that the spring constant did not vary for the range of loads placed on the beams. The maximum load in this test was 1 1/2 times as large as the biggest anticipated equivalent mass load.

b. Beam supports The simple support conditions for a simply supported beam are very difficult to satisfy. Three types of support were developed and tested before a satisfactory one was obtained.

PIN SUPPORTS The first supports consisted of two shallow holes drilled on opposite sides of the beam at each end where support was needed. Pointed set screws, which were threaded through tapped holes in the beam support brackets, were turned in until the points were snug against the beam. One of the support brackets had a similar pair of set screws at the top which provided lateral freedom. This method of support was identical to Stelson's (27) and was expected to provide nearly point support with little moment at the ends.

Some experiments were conducted which tested the repeatibility of the beams. These experiments showed that the tightness of the set screws and the reactions at the ends greatly effected the results. Since the support reactions vary during the experimental procedure, these supports were considered to be unacceptable.

BALL BEARINGS SUPPORTS The support brackets were rebuilt using ball bearings. The left hand support contained two ball bearings mounted on a shaft with a hole in the center. The beam was bolted to the shaft. The right support was similar except that two additional ball bearings were used to provide lateral motion. When these supports were new, they appeared to operate quite well.

As the bearings were used, they began to operate as if dirt were in them, but they could be freed easily by rotation and by cleaning with compressed air. The unfavorable behavior of the bearings would return after a few minutes of operation. This, coupled with poor repeatibility as they became older, indicated that the ball bearings were wearing small grooves in the races due to the oscillatory motion. Hence, the ball bearings were considered to be contributing to the experimental errors by changing the end conditions of the beams during the experiments.

The ball bearings were finally discarded when one of the bearings produced a very audible clatter which indicated that the inner race as well as the end of the beam was vibrating.

ELASTIC SUPPORTS The elastic support consisted of a short cantilevered beam with its longitudinal axis vertical. The end of this cantilever was rigidly attached to the end of the vibrating beam.

It was thought that the cantilever should be as flexible as possible in the flexural sense, but as stiff as possible in the axial sense. From an elementary and simplified analysis (where all nonlinear terms were assumed to be of secondary importance), the spring constant for the elastically supported beam was found to be increased by a factor of $1/(1 - \frac{6K}{L_2})$ where

$$\frac{6K}{L_2} = \frac{0.750}{\left[1 + 2\left(\frac{E_2}{E_1}\right)\left(\frac{I_2}{L_2}\right)\left(\frac{L_1}{I_1}\right)\right]} \cdot$$

The subscripts of 1 and 2 refer to the cantilever and beam respectively. From this relationship, the ratio of I_2/L_2 to I_1/L_1 should be as large as possible. The final design of the cantilever was a thin steel banding strap with dimensions of 0.023 in. x 0.749 in. by 2.20 in. long.

This method of supporting the beam worked very well. It gave the most consistent results in repeatibility tests, the cleanest signal on the scope, and was not disturbed by a horizontal vibration of the beam which had to be generated by an outside influence. It is well to note that the influence of the type two pickup on the natural frequency of the beam was detected after the elastic supports were developed

3. Inner sphere

A photograph of the inner sphere is shown in Fig. 10. In designing this sphere, the principal considerations were strength, weight, accuracy, and ease of manufacture. The spheres used in studies of this type must, of course, be impervious to the fluids.

Figure 11 shows a cross section of the sphere. The technique used in constructing the spheres proceded in eight steps. 1. A number ten brass rod was threaded to the proper lengths. 2. A nominal five-inch diameter Styrofoam ball was pierced through the center with a smaller diameter rod. 3. Two copper washers were cut out, and three holes were drilled through each washer. Two heavy copper wires were soldered to the washers with hooks on one side. One washer was attached to the brass rod between two nuts and soldered to the rod. 4. The brass rod was carefully pushed through the styrofoam ball following the hole made in step 2. The other washer was attached to the rod by a single nut, and the nut was advanced until the washers were drawn into the ball far enough for the hookes to be flush with the spherical surface. 5. A template was machined on a lathe by cutting a five inch diameter hole in a square piece of Plexiglass. The Plexiglass was cut along a diameter. Mounting brackets were attached to the template which held the brass rod and sphere in place relative to the template. A handle was attached to the brass rod for turning the sphere, and the template was placed in a vise. 6. A batch of "hydrocal B-11" (a product of United States Gypson)

Fig. 10 Inner sphere and outer shell

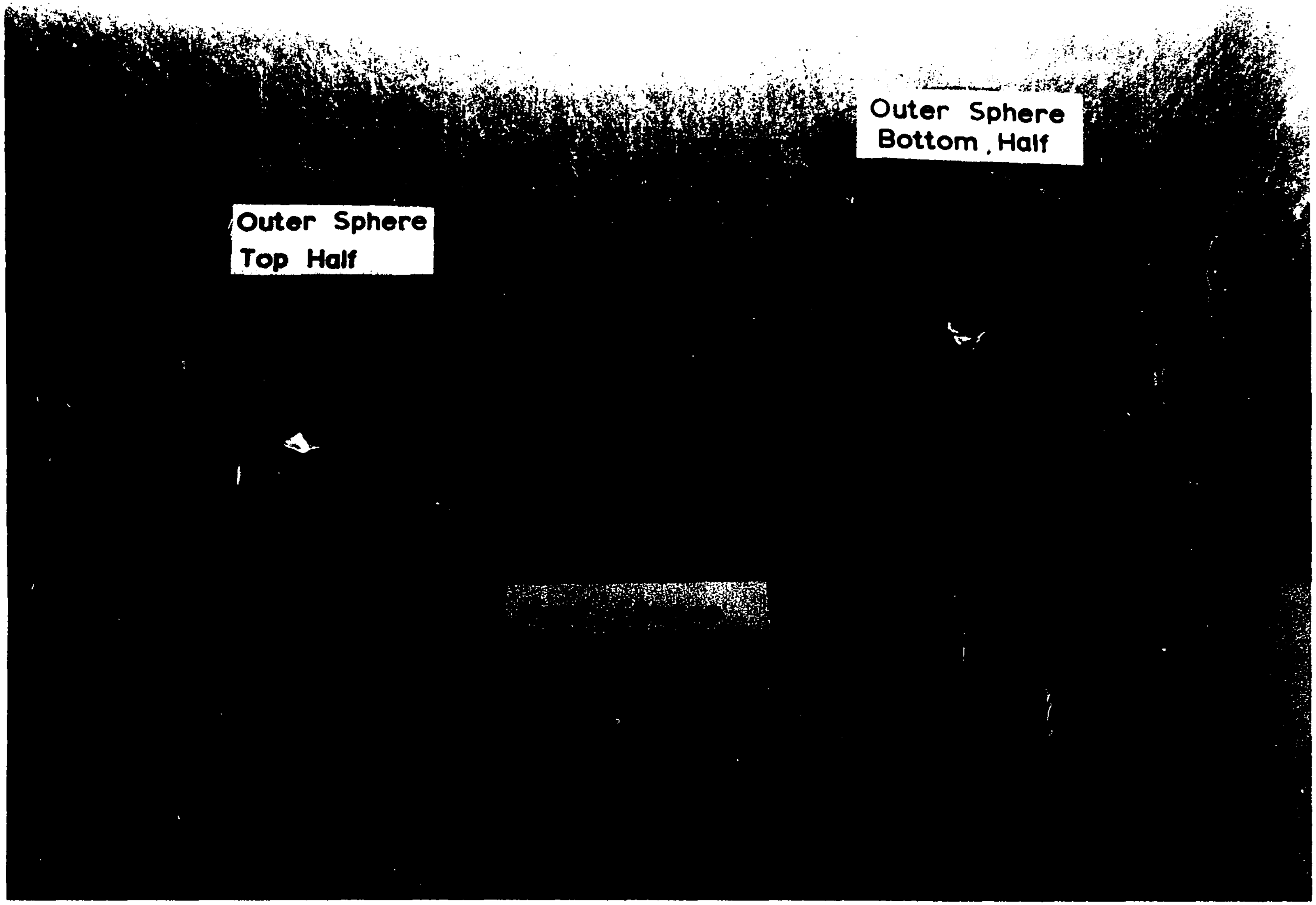
Outer Sphere
Top Half
Outer Sphere
Bottom, Half

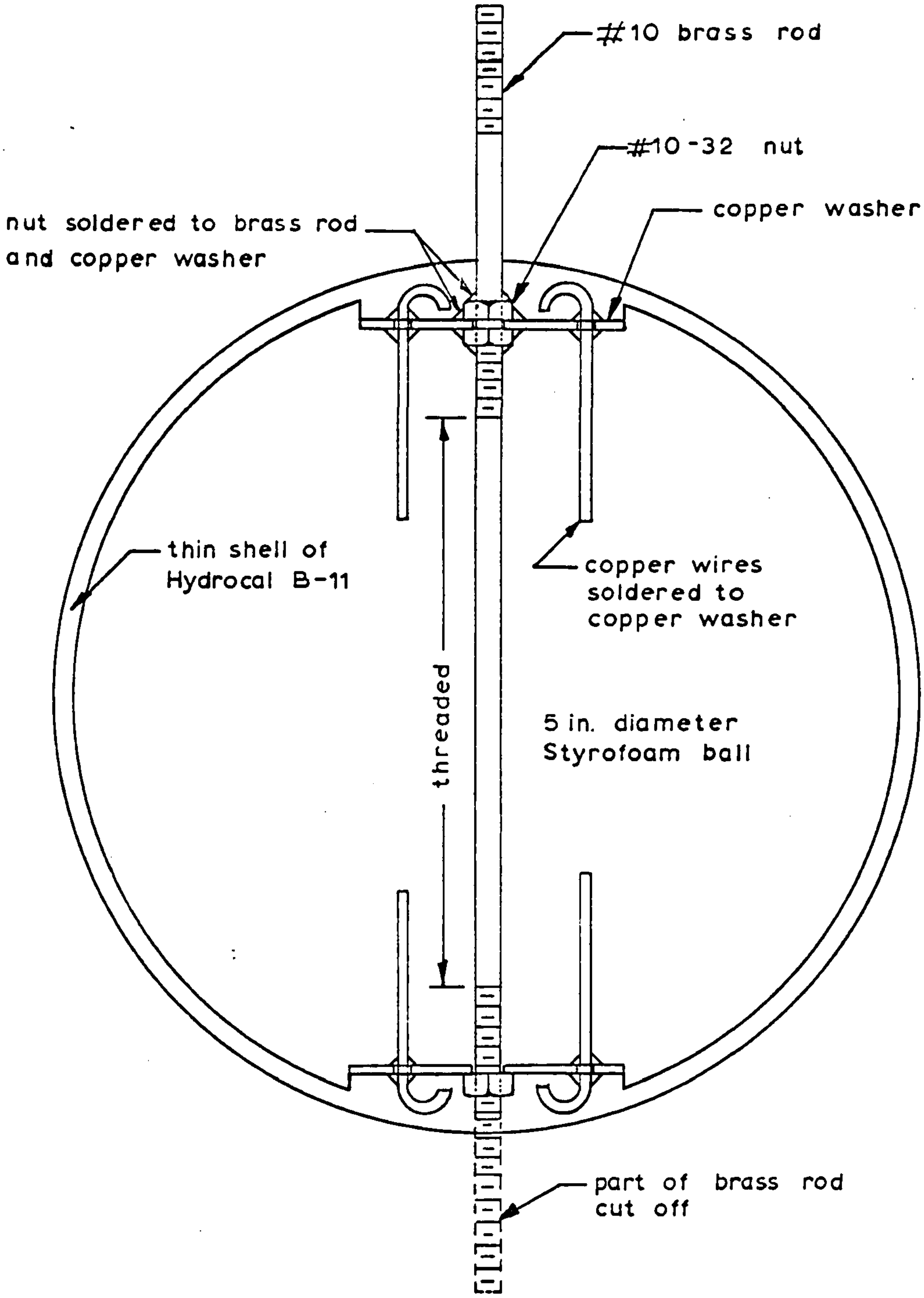

Fig. 11 Cross section of the inner sphere

and water was mixed to stiff consistency. This was applied to the surface of the Styrofoam ball which was slowly rotated past the template. After the first layer had been applied, water was added to thin the remaining mixture and to wet down the mixture already on the ball. The voids were filled and water freely added as the mixture began to set. 7. When the mixture was set, the sphere was quickly removed from the template, and the excess rod on one end was cut off and drilled out to a depth of about a 1/4 of an inch. The hole was filled with the "hydrocal" and smoothed over. 8. After drying for several days, the surface was given 10 to 12 coats of spar varnish with a light steel wool rub down between coats to remove any surface bumps due to dust in the air. The result was a smooth impervious surface.

This simple construction technique produced a sphere of high quality. The variation in diameter was less than 1 percent from the maximum to the minimum values measured. The average diameter was 5.00 inches and the weight of the sphere was 310 grams.

4. Outer spherical shell

A photograph of the outer shell is shown in Fig. 10. The outer shell design requirements were: to be separable, to be transparent for centering, to be strong, and to be arranged so the test fluid could be easily admitted and withdrawn. The first two requirements eliminated the possibility of building the spherical part with the equipment available. The answer was found in the form of a child's toy called a "Butterfly Ball". On inquiry, the manufacturer supplied the clear acetate balls.

These acetate balls were too flexible so a Plexiglass frame was built to make them stronger and more rigid. A special cement for bonding Plexiglass to acetate was obtained.

Several difficulties were encountered in the construction of the outer shell. First, the special cement was too weak. "Duco household cement" was found to provide a much stronger bond. Second, leaks at the joint between the hemispheres were common. This was finally stopped by using "florists clay". Third, the acetate was very unstable and had a tendency to shrink. The spherical surface degenerated to approximately the same shape a thin membrane or balloon would take, had the membrane been stretched over an imaginary frame made of four equally spaced semi-circles. The majority of this shrinkage would take place in a period of about two weeks. Since the shrinkage was more severe with the "Duco" cement than with the special cement, it is suspected that one or more of the solvents in the "Duco" cement may be the cause. Fourth, the acetate shell was drawn away from the heavy ring where the two hemispheres joined. Fifth, the most serious problem was the low rigidity which the Plexiglass frame provided. This last effect is related to Pi term π_6 discussed in the dimensional analysis section.

5. Equivalent mass weights

The initial apparatus used to determine the equivalent mass consisted of a thin shell cylindrical container with a number ten brass rod running from the beam to the bottom of the container which was reinforced by a 1/4 inch steel plate. The container was filled with the correct amount of lead shot in the experiment. It was observed that a phase shift occurred when the amplitude of vibration increased and that the bottom of the container was flexing. To correct this, a better weight was constructed. The new weight was made from the end cap of a two inch water pipe. Enough lead was melted and poured into it to give the basic unit a weight of about 1,600 grams. There was enough room on top to hold about 500 grams in the form of lead shot. A second lead weight of about 450 grams was cast which could be bolted to the bottom of the basic unit. This gave a range of 1,600 to over 2,500 grams with a much smaller portion of the weight being supplied by the lead shot. The new weight proved satisfactory.

6. Experimental Fluids

Originally, the intention was to use five fluids. A description of these is given in Table 2. In the preliminary tests, fluid number II was sufficiently viscous to produce nearly critical damping, and no useful information could be obtained from the damped oscillation trace. Hence, fluid number II was not used in the remainder of the experiments.

Table 2. Experimental fluids

Fluid number	Composition
I	tap water
II	140 weight aircraft engine oil
III	50% 140 weight aircraft engine oil 50% SAE 10 motor oil
IV	95% SAE 10 motor oil 5% Kerosene
V	40% SAE 10 motor oil 60% Kerosene

Standard values for the kinematic viscosity of water were used for tap water. For the other fluids which are liquid petroleum products, the A.S.T.M. standard test (D341) was used where the kinematic viscosity was converted from "Saybolt Universal Seconds" to units of square feet per second. The density of the fluid was measured by using a hydrometer during each experiment.

D. Final Experimental Procedure

The final experimental procedure consisted of 10 steps as follows:

1. The moving support was raised to its up position. The inner sphere was attached to the beam and centered vertically and horizontally.
2. The fluid was admitted, and its temperature recorded. When the fluid level was near the top of the inner sphere, the vertical position of the inner sphere was checked. (Experiments without the fluid showed that vertical centering could be done without influencing the horizontal position.)
3. The Brush amplifiers were balanced, and the natural frequency was determined by slowly adjusting the oscillator until a circle or an ellipse appeared on the scope. The amplitude of oscillation was increased until a slight additional shift occurred. This gave the limit at which π_4 began to influence the results, and the maximum amplitude used in the remaining steps was below this value.
4. The balance of the Brush amplifier #2 was checked. When this amplifier was in perfect balance and the oscillator was set

precisely at the natural frequency, the circle or ellipse on the scope reduced to a semi-circle or parabola when the OPERATE switch on the amplifier was turned to the BALANCE position. This provided a check on the accuracy of the oscillator setting indicating with certainty the point at which the phase shift was 90 degrees. The power to the speaker was cut off. The recording pen was centered on the paper, and the OPERATE switch on the Brush amplifier #2 was again turned to the BALANCE position. As a final check on the accuracy of the driving frequency, the power was turned on and the resulting semi-circle or parabola was observed on the scope. If no detectable shift from 90 degrees occurred during the increase of amplitude, it was concluded that the oscillator was set at the natural frequency.

5. Two damped oscillation traces and one natural frequency trace were recorded. (PROCEDURES I AND II)
6. The fluid was drained and the inner sphere was detached from the beam. The moving support was lowered to its down position, and the equivalent mass container was attached to the beam.
7. The mass in the equivalent mass container was either increased or decreased until the beam and mass combination had a natural frequency which was the same as the oscillator setting. The procedure used in step 4 to check the accuracy of the oscillator setting was also used to check the accuracy of the equivalent mass. When everything appeared satisfactory, two damped traces

were recorded. (PROCEDURES III AND IV) It should be pointed out that this damped frequency was used to cross check the natural frequency of the beam and of the sphere since the combined damping of the beam and equivalent mass container was so small.

8. The mass m_a was attached and a damped trace was recorded. (PROCEDURE V)

9. The equivalent mass M_e was removed from the beam and weighed on a torsion balance.

10. Either beam or the fluid was changed in order to vary Stokes' number.

The volume of the outer shell was determined before and after each series of tests. The inner sphere was in place during this measurement. Water was admitted and then removed. The volume of water between the spheres was collected in a graduate and weighed. This was repeated three or four times.

The weights were averaged, and the volume between the spheres was determined by dividing the averaged weight of water by its corresponding specific weight. To obtain the volume of the outer sphere, the volume of the inner sphere which was determined in a similar fashion was added. The results of these volume measurements over a period of time is given in Table 3 for the outer shell used in Series III, V, and VI. Note that the outer shell shrank with age.

Table 3. Volume measurements of outer shell IV

Date	Time	Series	Volume cm^3	Dia. in. (based on vol.)	Dia. in. (at hemisphere joint)
June 5*	a.m.	III	2,740.6	6.835	6.897
June 6	p.m.	III	2,729.5	6.826	6.878
July 2	a.m.	V	2,689.7	6.792	6.875
July 4	p.m.	V	2,670.2	6.776	6.872
July 10	a.m.	VI	2,676.0	6.781	6.880
July 10	p.m.	VI	2,670.4	6.776	6.860

*The outer shell was new on June 3

V. RESULTS

The results of the experimental program are given as three series of data which are labeled III, V, and VI. Series I, II, and IV are not shown because these were preliminary tests with the apparatus where technical problems caused scatter and are not considered as reliable. The three series presented show some of the effects of the apparatus with a steady improvement in the data.

A. Series III

The data for series III are shown in Figs. 12 and 13. The operating conditions for these tests were: ball bearing supports, new outer shell (see Table 3 for volume) and type two vibration pickup mounted at the center of the beam.

1. Added mass coefficient

The added mass coefficient is plotted against Stokes' number in Fig. 12. The scatter in this data is considerable, but it follows in a very persistent pattern in three out of four fluids. When the fluid is water ($2x10^5 < \frac{\omega a^2}{\nu} < 8x10^5$), three beams (4, 9, and 12) were used. Their respective errors were approximately 1, 5.6, and 12.8 per cent with respect to Stokes' solutionfor $\lambda = 0.730$ or curve A. If the frequency of vibration for each beam is squared, and the ratio of the frequency squared for each beam is taken with respect to that of beam 4, the result is 1, 5.3, and 17.2. The correlation is not perfect, but the influence of an ω^2 term appeared feasible. This observation is supported by the fact that Curves A, B, and C follow the experimental points for beams 4, 9, and 12 respectively with reasonable accuracy.

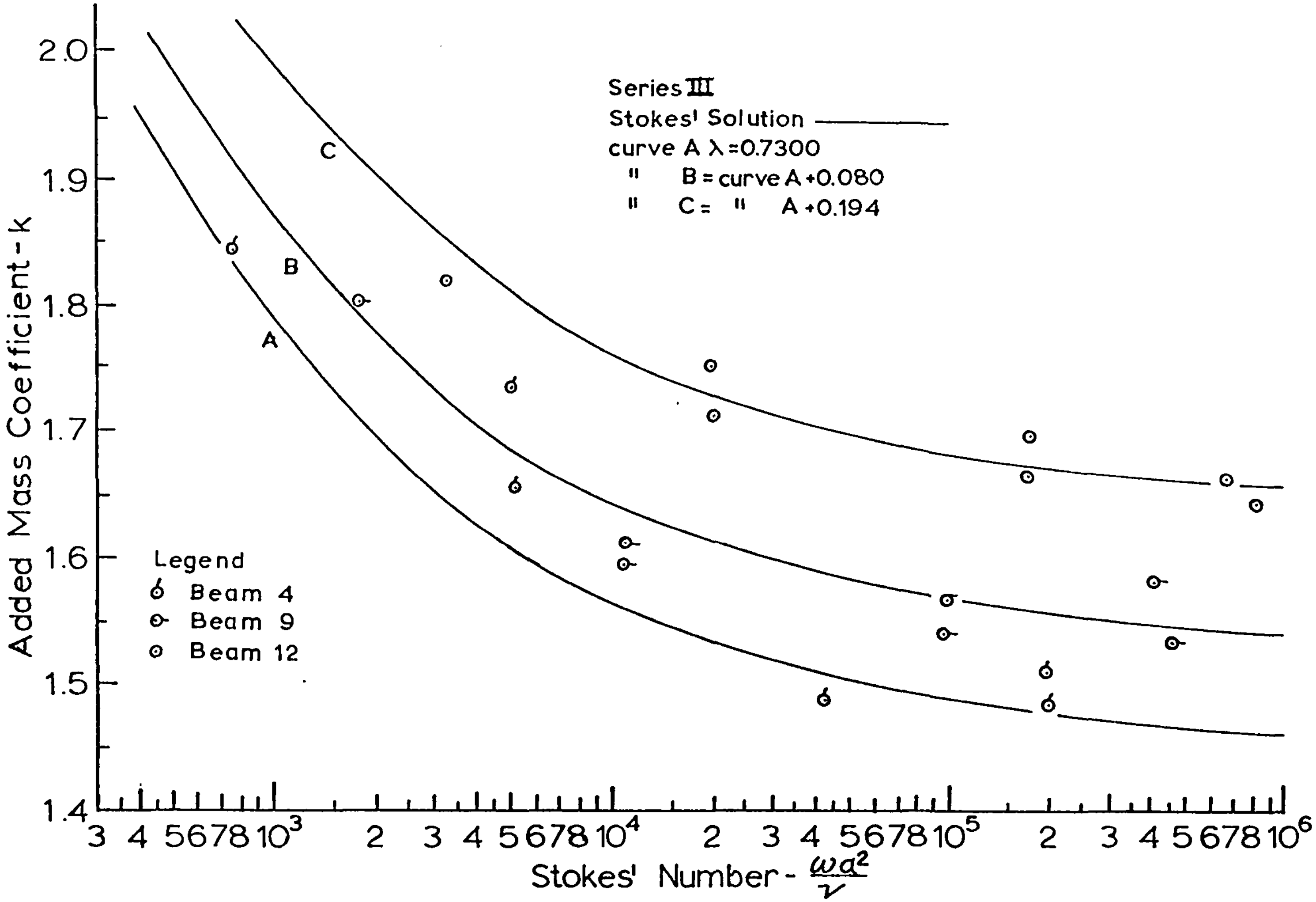

Fig. 12. Added mass coefficient vs. Stokes' number for series III

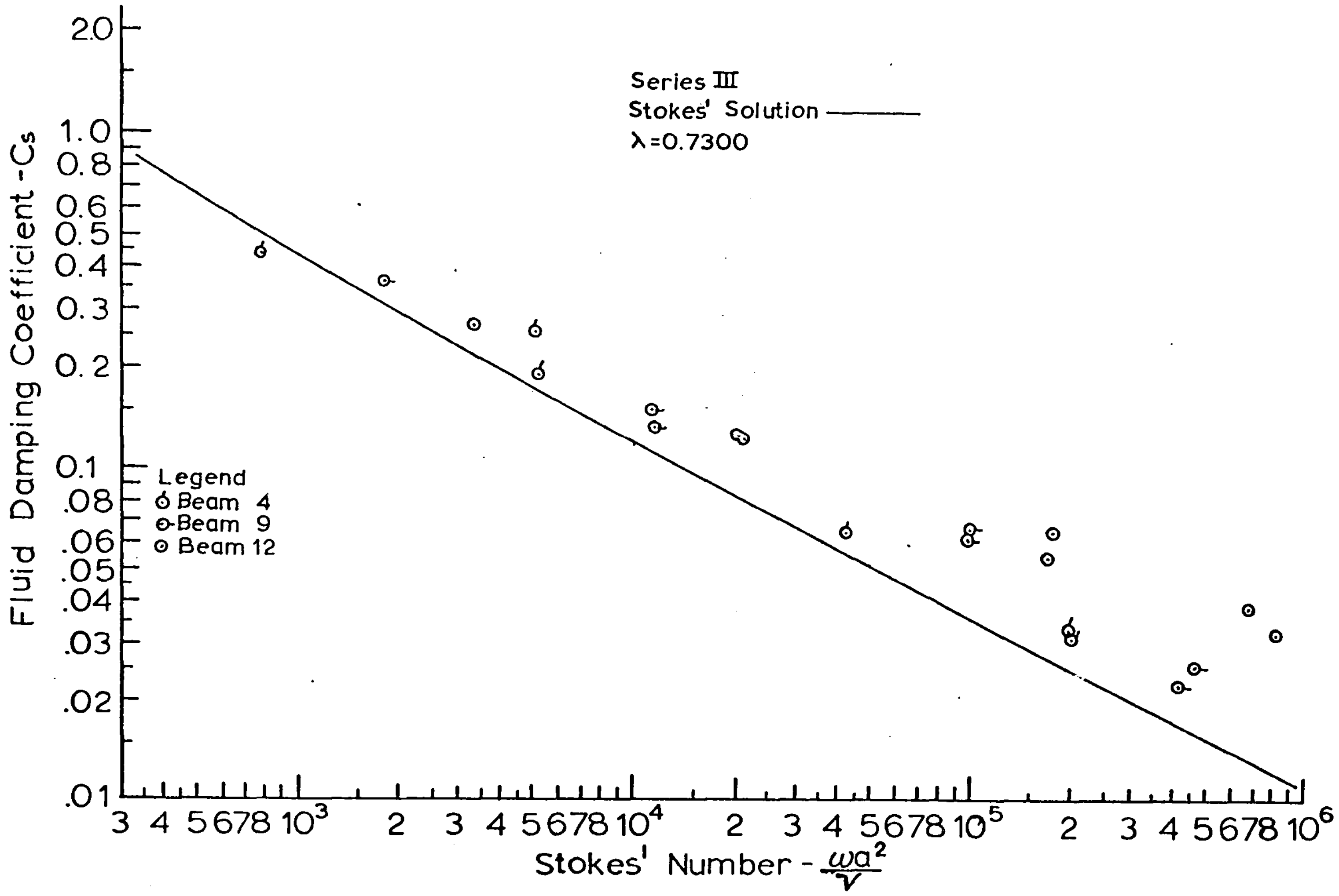

Fig. 13 Fluid damping coefficient vs. Stokes' number for series III

It was at this point that the dimensional analysis was re-examined to see if any significant variables had been omitted. The result of this examination was the addition of π_6. An examination of the pressure distribution acting on the outer shell indicated that the fluctuating pressure was dependent on $\rho\omega^2\bar{\delta}$. This, coupled with a realization that the relative stiffness of the supporting frame was dependent on a term similar to π_6, indicated a need to stiffen the outer shell and the supporting frame. Two 2 in. x 6 in. planks were wedged between the floor and the top support with one plank at the center of the various positions for each of the support brackets, and a 2 in. x 4 in. plank was wedged between the floor and the center of the moving support during each run. Four clamps were used to stiffen the connection between the hemispheres. This required the addition of spacers to prevent damage to the acetate connection.

2. Fluid damping coefficient

Values for the fluid damping coefficient are plotted in Fig. 13. The general trend of Stokes' solution is followed, but most of the points are high. The repeatibility was satisfactory.

B. Series V

The data of series V are shown in Fig. 14 and 15. The operating conditions for these tests were: elastic supports for the beam, outer shell clamped at joint, type two vibration pickup, and wooden supports for top and moving support, respectively.

1. Added mass coefficient

The added mass coefficient is plotted in Fig. 14. The definite trend which was associated with the beams in series III seems to be

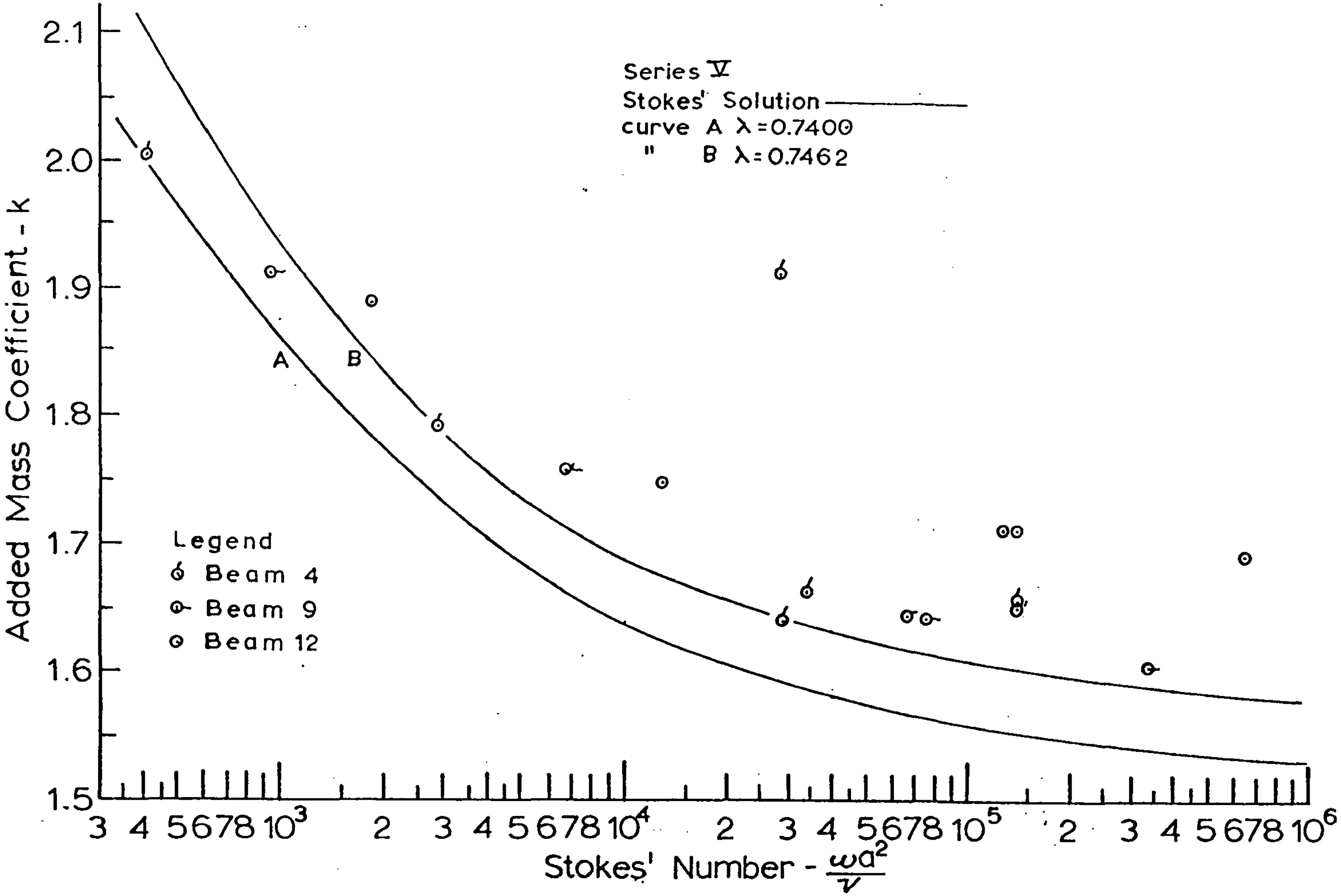

Fig. 14 Added mass coefficient vs Stokes' number for series V

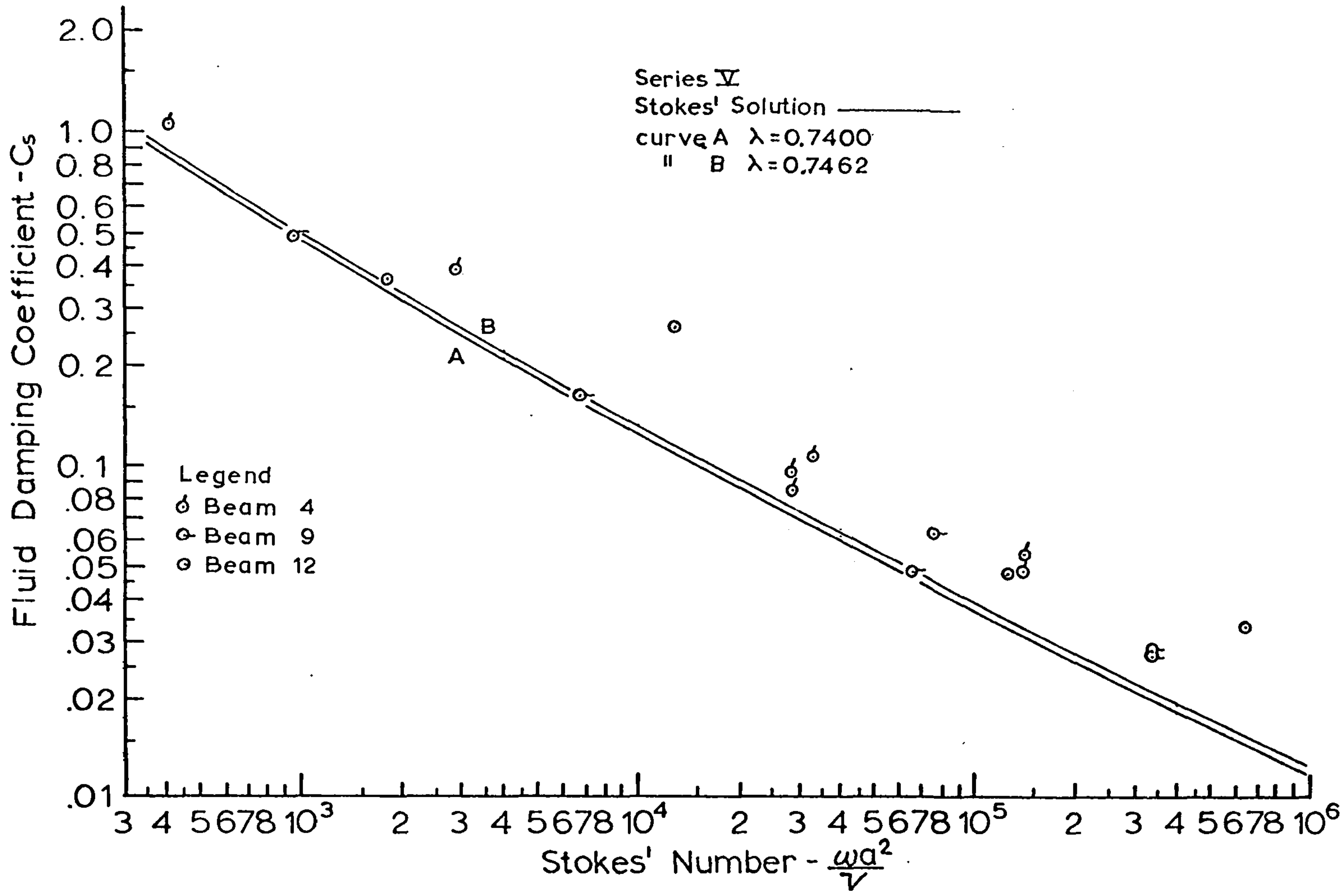

Fig. 15 Fluid damping coefficient vs. Stokes' number for series V

reduced with the exception of beam 12. The rigidity of the shell was too low for this beam. It was observed during the test, particularly with the less viscous fluids, that the fluid was moving in and out of the space between the two clamping rings at the joint of the hemispheres. This, at first, was thought to be the entire source of error, but during a repeatibility test with beam 4, the effect of the position of the type two vibration pickup was detected. These problems were corrected by using florist clay and by putting SR-4 strain gages on the beams

2. Fluid damping coefficient

Values for the fluid damping coefficient are plotted in Fig. 15. A comparison of the data in this series with the previous series, shows that the general scatter is reduced. The largest errors generally belong to beam 12.

C. Series VI

The last series of the data is plotted in Figs. 16 and 17. The operating conditions for these tests were: elastic supports, outer shell five weeks old and clamped at joint, florist clay used to seal joint rather than electrical tape, SR-4 gages on beams for pickups, and 2 in x 6 in. and 2 in. x 4 in. wooden supports. Beam 7 was added to the other three beams for this series as a check on beams 4 and 9. The values of added mass and damping coefficients for beam 12 repeated previous data and are not plotted in Figs. 16 and 17 since the rigidity effects associated with the Pi term π_6 could not be entirely eliminated from the apparatus. Hence, the data of beam 12 were not considered to be typical of the phenomenon.

During a pre-series test of equipment, it was found that beam 4 would exhibit a slight phase shift with changes in amplitude when the equivalent mass was attached. The addition of mass at the center of the beam reduced this phase shift considerably when vibrating at resonance. Hence, a 1039 gram mass was attached to the center of each beam for this series.

There was some concern about the oscillator drifting during the experiment when operating on its lowest scale for beam 4. This was investigated before this series was started, and it was found that the drifting was considerable during the first ten minutes of the warm up period. After half an hour, the drifting was negligible.

1. <u>Added mass coefficient</u>

The added mass coefficient is plotted in Fig. 16. From this plot it is seen that all of the points lie above Stokes' solution for the measured value of $\lambda = 0.740$ based on volumes. However, since the outer shell was in a condition similar to the stretched membrane, it is not unreasonable to suspect that the boundaries are somewhat closer at points. A second theoretical solution was calculated for $\lambda = 0.7462$ where the curve would pass through the last three points on the right. It is seen that nearly every point lies between the two curves. The percent of error for each data point (from left to right in Fig. 16) with respect to both curves is given in Table 4. From this table, it is seen that the agreement is better than it appears in Fig. 16 which has an expanded vertical scale.

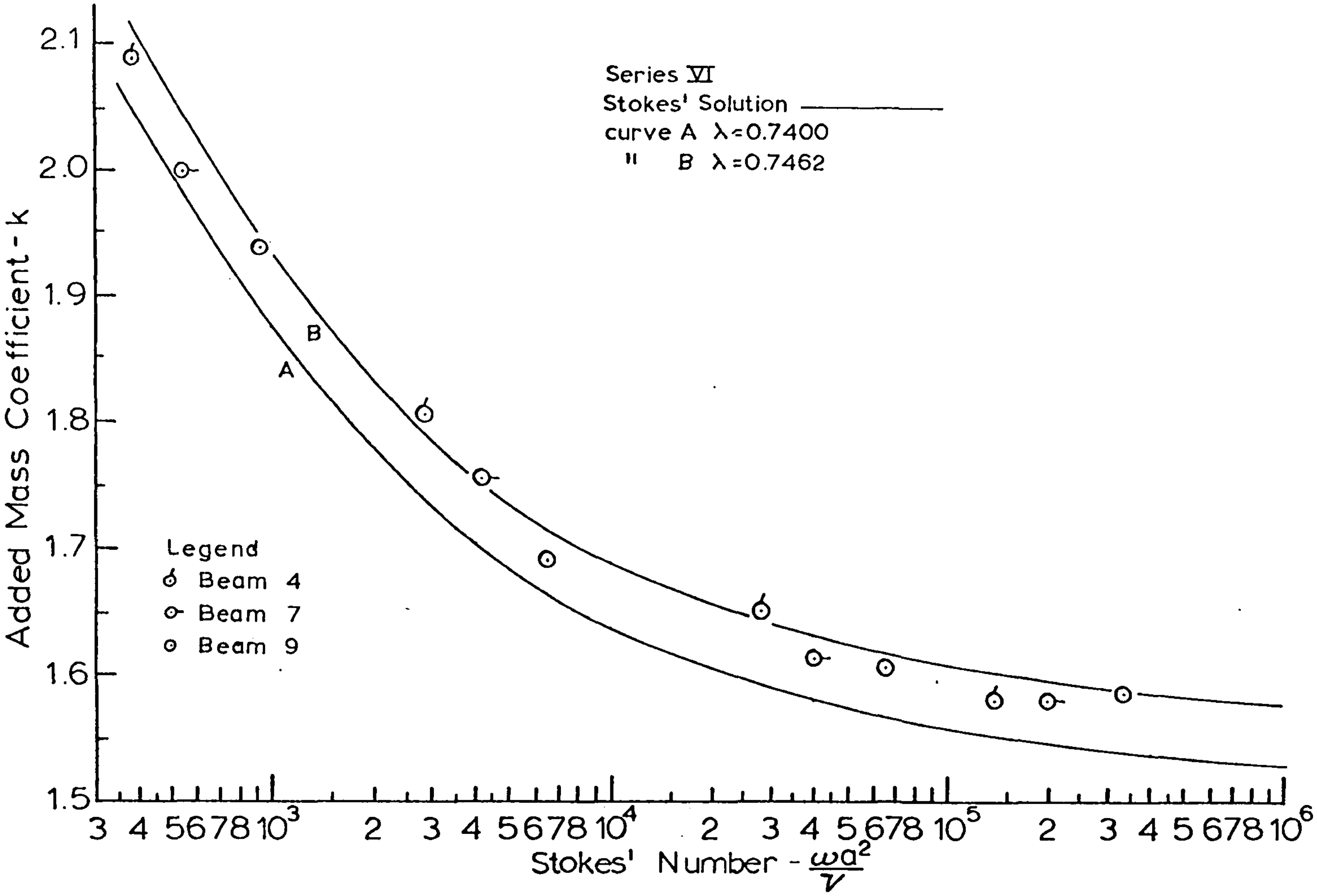

Fig. 16 Added mass coefficient vs Stokes' number for series VI

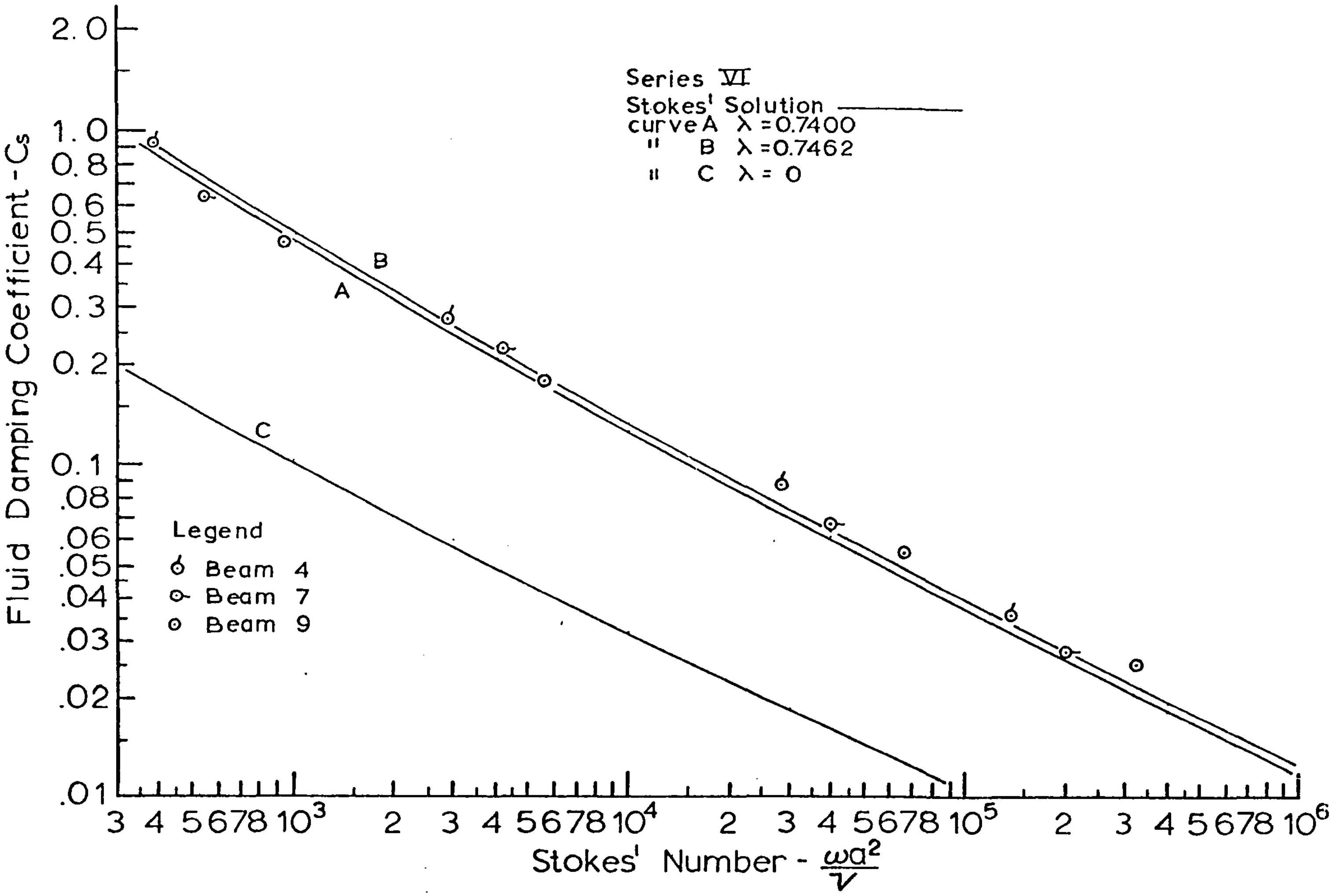

Fig. 17 Fluid damping coefficient vs. Stokes' number for series VI

The sensitivity of the added mass coefficient to slight errors in determining λ cannot be underestimated. From the potential flow solution, the added mass coefficient is given by

$$k_p = \frac{1}{2}\left(\frac{1 + 2\lambda^3}{1 - \lambda^3}\right) \tag{41}$$

where the form given in Eq. 25-a is written in terms of λ. The

Table 4. Errors in added mass coefficients for series VI

Beam number	% error $\lambda = 0.740$	%error $\lambda = 0.7462$
4	+1.46	-1.14
7	+0.55	-2.26
9	+1.96	-1.03
4	+3.74	+0.73
7	+3.17	+0.17
9	+1.44	-1.58
4	+3.57	+0.79
7	+2.15	-0.67
9	+2.80	0
4	+2.06	-0.81
7	+2.40	-0.50
9	+3.25	+0.19
Ave	+2.38	-0.51

potential flow solution increases by 4.6 per cent when λ increases from 0.730 to 0.740 (an increase of 1.37 percent). The increase obtained from Stokes' viscous flow solution is slightly greater due to the viscous effects. The values of λ ranged from 0.735 to 0.741 for series VI.

These values depend on whether the volumetric diameters or the measured diameters were used and have a range of values of about 0.81 percent. Hence, the average errors shown in Table 4 are within the bounds of a half percent error in measuring the diameters.

2. Fluid damping coefficient

The fluid damping coefficient is shown in Fig. 17 for series VI. The general agreement of the experimental data with Stokes' solution is good considering the number of assumptions necessary to evaluate this data and Stokes' assumption of steady oscillatory motion in arriving at the theoretical solution.

The change in the fluid damping coefficient for small changes in λ is small. In order to illustrate this lack of sensitivity to λ, a third curve for $\lambda = 0$ is plotted in this figure.

VI. SUMMARY AND CONCLUSIONS

Based on the general agreement between the theory and experimental results, it is concluded that the viscous flow solution will accurately predict the added mass coefficient and the fluid damping coefficient if the amplitudes of motion are small compared to the inner radius or gap between the spheres, and if the boundaries are sufficiently stiff or rigid to satisfy the specified boundary conditions. The Stokes' number provides a good measure for determining when the viscous effects are important and whether or not these effects should be included in the analysis of a given problem. From Fig. 16 and Stokes' solution (for the added mass coefficient), it can be seen that the viscous solution is asymptotically approaching the constant value which is given by the potential solution in Eq. 41. When Stokes' number is approximately 1×10^5 or higher, these two solutions only differ by a small amount. For other shapes and sizes, the particular value of Stokes' number for the viscous effects to be negligible is dependent on the length term used. The viscous effects must be included in the analysis of a given problem where damping is considered to be important.

The differential equation of motion of the inner sphere, as given by Eq. 26-a, can be treated as a second-order differential equation with constant coefficients when Stokes' number is constant. For a given system, the plot of amplitude of vibration and phase shift versus the frequency ratio may be obtained in the usual manner if the added mass and the damping coefficient variations are taken into account. If the forcing function is expressed in a Fourier series, the response of the second-order differential equation can be calculated by using standard techniques provided the correct added mass and fluid damping coefficients are used with each frequency in the Fourier expansion.

The boundary layer on the inner sphere is of greatest importance since it is this thin layer of fluid which produces damping and the variation of the added mass coefficient and the fluid damping coefficient with respect to Stokes' number. This boundary layer is quite different from the boundary layer which is associated with a constant rectilinear velocity. In the oscillatory case, the boundary layer is continuously being created and destroyed in the sense that the motion is periodically reversing direction. Hence, the separation of the boundary layer should not take place unless the amplitude of motion and the period of oscillation are large. It is estimated by means of Eq. 12* that the boundary layer thickness is approximately one eighth of an inch or less for Stokes' numbers greater than 10,000. Turbulence appears to have either no net effect or a second-order effect which is less than the equipment and experimental technique can detect.

The reason for the good agreement between experimental results and potential flow analysis which was obtained in several reported experimental investigations is that these experiments were conducted in water and other low viscosity fluids which give high Stokes' numbers. With high Stokes' numbers, the viscous effects are negligible and results would easily be within one per cent of the potential flow solutions. Hence, the conclusion has been frequently drawn that the added mass coefficient is constant and equal to the potential theory values. This is not actually the case as demonstrated by the results of this investigation, for the added mass coefficient and the fluid damping coefficient are dependent on Stokes' number. It is expected that this conclusion would be valid for other shapes as well as spheres.

From consideration of Eqs. 1-a, 13*, and 26-a, the experimental results and observations during the experimental investigation, and the dimensional analysis, it is concluded that the differential equation of motion for other shapes of rigid bodies performing rectilinear oscillations will be a second-order differential equation with varying coefficients. The variation of these coefficients is due to the added mass coefficient and the fluid damping coefficient which are dependent on the geometrical configuration of the rigid body and the envelope, the Stokes' number, the amplitude of oscillation, and the rigidity of the bodies in the vibrating system.

VII. SUGGESTIONS FOR FURTHER STUDY

Research into one problem usually creates an awareness of other problems which need to be investigated. Some of the more interesting problems which are thought to be of sufficient importance to warrant further study are the following.

1. Study practical means or procedures which can be used to alter potential flow solutions in such a way that the viscous effects can be approximated for oscillating motion. Eqs. 12* and 13* may provide the key for this alteration.
2. Study the effects of the rigidity of the outer shell or more generally the effects of an elastic boundary.
3. Study the effects of turbulence on added mass.
4. Study the effects of amplitude on added mass coefficient and fluid damping coefficient. Szebehely (34) has shown this effect to exist in his studies on the damping of a spheroid.
5. Study rotational added mass or added moments of inertia coefficients and fluid damping coefficients.
6. Study added mass coefficients and fluid damping coefficients with a vibrating body in an oscillating flow. This has been done for stationary cylinders and flat plates by Keulegan (14) and McNown (18).
7. Study the possibility of superposition of two separate orthogonal vibrations.

VIII. ACKNOWLEDGEMENTS

The author takes this opportunity to express his sincere appreciation to Dr. Donald F. Young whose advice, encouragement, and guidance were invaluable during the course of this investigation.

The author wishes to thank his wife, Dee, whose encouragement and understanding made this work possible.

IX. BIBLIOGRAPHY

1. Baily, F. On the correction of a pendulum for the reduction to a vacuum: together with some anomalies observed in pendulum experiments. Roy. Soc. Lond. Trans. 1832: 399-492. 1832.

2. Basset, A.B. On the motion of a sphere in a viscous liquid. Roy. Soc. Lond. Trans. 179: 43-63. 1888.

3. Basset,A.B. On the motion of two spheres in a liquid, and allied problems. Lond. Math. Soc. Proc. 18: 369-377. 1887.

4. Bessel, F.W. Untersuchungen über die länge des einfachen secundenpendels. Akad. d. Wissensch. Berlin Abhandl. d. Math. u. Phys. Klas.: 1-256. 1826.

5. Boussinesq, M.J. Sur la résistance d'une sphère solide. Acad. d. Sci. Comp. Rend. 100: 935-937. 1885.

6. Cook, G. An experimental determination of the inertia of a sphere moving in a fluid. Lond., Edin., Dub. Phil. Mag. Jour. Sci. Ser. 6, 39: 350-352. 1920.

7. Darwin, C. Note on hydrodynamics. Camb. Phil. Soc. Proc. 49: 342-354. 1953.

8. DuBaut, C. Principes d' hydraulic. 2nd ed. Vol. 2. Paris, France. 1786. (1st ed. in 1779) Original not available; cited and described in Baily, F. On the correction of a pendulum for the reduction to a vacuum: together with some anomalies observed in pendulum experiments. Roy. Soc. Lond. Trans. 1832: 458-461. 1832.

9. Eskinazi, S. Principles of fluid mechanics. Boston, Mass., Allyn and Bacon, Inc. 1962.

10. Green, G. Researches on the vibration of pendulums in fluid media. Roy. Soc. Edin. Trans. 13: 54-62. 1836.

11. Haberman, W.L. The potential problem of a sphere inside a circular cylinder. David Taylor Model Basin (Washington 7, D.C.) Report No. 1563. 1961.

12. Hicks, W.M. On the motion of two spheres in a fluid. Roy. Soc. Lond. Trans. Ser. A, 171: 455-492. 1880.

13. Imlay, F.H. The complete expressions for "added mass" of a rigid body moving in an ideal fluid. David Taylor Model Basin (Washington 7, D.C.) Report No. 1528. 1961.

14. Keulegan, G.H. and Carpenter, L.H. Forces on cylinders and plates in an oscillating fluid. Nat'l. Bur. Stand. Jour. Res. Ser. 5, 60: 423-440. 1958.

15. Krishnayer, N.C. An experimental determination of the inertia of a sphere vibrating in a liquid. Lond., Edin., Dub. Phil. Mag. Jour. Sci. Ser. 6, 46: 1049-1053. 1923.

16. Lamb, H. Hydrodynamics. 6th ed. New York, N.Y., Dover Publications. 1945.

17. McEwen, G.F. The measurement of the frictional force exerted on a sphere by a viscous fluid, when the center of the sphere performs small periodic oscillations along a straight line. Phys. Rev. Ser. 5, 33: 492-511. 1911.

18. McNown, J.S. and Keulegan, G.H. Vortex formation and resistance in periodic motion. Am. Soc. Civ. Eng. Proc. 85, Jour. Eng. Mech. Div. 1: 1-6. 1959.

19. Meyer, O.E. Über die pendelnde bewegung einer kugel unter dem einflusse der inneren reibung des umgebenden mediums. Jour. fur d. reine und angew. Math. 73: 31-68. 1871.

20. Milne-Thomson, L.M. Theoretical hydrodynamics. 4th ed. New York, N.Y., The Macmillan Co. 1960.

21. Murphy, G. Similitude in engineering. New York, N.Y., The Ronald Press Co. 1950.

22. Pipes, L.A. Applied mathematics for engineers and physicists. 2nd ed. New York, N.Y., McGraw-Hill Book Co., Inc. 1958.

23. Polya, G. A minimum problem about the motion of a solid through a fluid. Nat'l. Acad. Sci. (U.S.A.) Proc. 33: 218-221. 1947.

24. Rayleigh, Lord. On the motion of solid bodies through a viscous liquid. Lond., Edin., Dub. Phil. Mag. Jour. Sci. Ser. 6, 21: 679-711. 1911.

25. Sabine, E. On the reduction to a vacuum of the vibrations of an invariable pendulum. Roy. Soc. Lond. Trans. 1829: 207-239. 1829.

26. Sarpkaya, T. Added mass of lenses and parallel plates. Am. Soc. Civ. Eng. Proc. 86, Jour. Eng. Mech. Div. 3: 141-152. 1960.

27. Stelson, T.E. Acceleration of bodies in fluids: a study of virtual mass. Unpublished Doctor of Science thesis. Pittsburgh, Penn., Library, Carnegie Institute of Technology. 1952.

28. Stelson, T.E. and Mavis, F.T. Virtual mass and acceleration in fluids. Am. Soc. Civ. Eng. Proc. 81, Separate No. 670: 1-9. 1955.

29. Stokes, G.G. On some cases of fluid motion. Camb. Phil. Soc. Trans. 8: 105-137. 1843.

30. Stokes, G.G. Mathematical and physical papers. Vol. 1. Cambridge, England, Cambridge University Press. 1880.

31. Stokes, G.G. On the effect of internal friction of fluids on the motion of pendulums. Camb. Phil. Soc. Trans. 9: 8-106. 1850.

32. Stokes, G.G. Mathematical and physical papers. Vol. 3. Cambridge, England, Cambridge University Press. 1901.

33. Streeter, V.L. Fluid dynamics. New York, N.Y., McGraw-Hill Book Co., Inc. 1948.

34. Szebehely, V.G. Oscillatory motion of a spheroid. Nat'l. Cong. App. Mech. (U.S.) 2: 771-775. 1954.

35. Valensi, J. and Clarion, C. Oscillations amourties d'une sphère dans un fluide visqueux. Inter. Cong. Theo. Appl. Mech., Istanbul, 1952, Proc. 8: 274. 1952.

X. APPENDIX A. THE VISCOUS FLOW SOLUTION

The viscous flow solution for two concentric spheres was developed by Stokes (31, 32) in 1850. The starred equation numbers in this section correspond to those of Stokes'. Seven assumptions were made by Stokes in order to obtain this solution.

The four initial assumptions were:

1. "The motion is supposed very small, on which account it will be allowable to neglect the terms which involve the square of the velocity." This is equivalent to neglecting the convective acceleration terms and corresponds to the usual viscous or slow flow assumption. As previously noted in conclusion number 2 of the potential flow solution, the convective terms do not enter into the resultant fluid force on a sphere if the sin θ cos θ product is formed in each of these terms. Hence, the potential flow solution indicates that the viscous or slow flow assumption is justifiable for a sphere. Apparently Stokes was not aware that the convective terms would drop out of the solution.
2. "The motion that we have got to deal with is such.....that we may treat the fluid as incompressible....".
3. The effect of the body forces due to gravity "is simply a force equal to the weight of fluid displaced, and acting vertically upwards through the centre of gravity of the volume". This assumption is similar to conclusion number 1 from the potential flow analysis and equivalent to neglecting the body forces in the equations of motion of the fluid.

Stokes was solving the problem of a sphere swinging as a simple pendulum. He considered the rotation of the sphere to be a second-order quantity, and the curved path of the center to be rectilinear. Thus, his fourth assumption: "The problem, then, reduces itself to this. The centre of a sphere performs small periodic oscillations along a right line, the sphere itself having a motion of translation simply: it is required to determine the motion of the surrounding fluid." From these four assumptions, the axisymmetric equations of motion for a viscous fluid are developed.

The axisymmetric equations of motion for a viscous fluid in the absence of body forces and the convective acceleration terms are obtained from the Navier-Stokes equations (see Eq. 7, 7-a, and 7-b) by a transformation of coordinates. He begins by stating, "Let the mean position of the centre of the sphere be taken for origin, and the direction of its motion for the axis of x, so that the motion of the fluid is symmetrical with respect to this axis. Let ϖ be the perpendicular let fall from any point on the axis of x, q the velocity in the direction of ϖ, ω the angle between the line ϖ and the plane of xy. Then P, u, and q will be functions of x, ϖ, and t, and we shall have $v = q \cos \omega$, $w = q \sin \omega$, $y = \varpi \cos \omega$, $z = \varpi \sin \omega$, whence $\varpi^2 = y^2 + z^2$, $\omega = \tan^{-1} \frac{z}{y}$."

If the proper differentiations are performed, Eqs. 7, 7-a, and 7-b transform to

$$\frac{dP}{dx} = \mu \left(\frac{d^2u}{dx^2} + \frac{d^2u}{d\varpi^2} + \frac{1}{\varpi} \frac{du}{d\varpi} \right) - \rho \frac{du}{dt} \qquad (16*)$$

$$\frac{dP}{d\bar{\omega}} = \mu\left(\frac{d^2q}{dx^2} + \frac{d^2q}{d\bar{\omega}^2} + \frac{1}{\bar{\omega}}\frac{dq}{d\bar{\omega}} - \frac{q}{\bar{\omega}^2}\right) - \rho\frac{dq}{dt}, \qquad (17^*)$$

and the continuity equation (see Eq. 8) transforms to

$$\frac{du}{dx} + \frac{dq}{d\bar{\omega}} + \frac{q}{\bar{\omega}} = 0 \ . \qquad (18^*)$$

If the stream function ψ is expressed as

$$d\,\psi = \bar{\omega}\ (u\,d\,\bar{\omega} - q dx) = \frac{\partial\psi}{\partial x}\,dx + \frac{\partial\psi}{\partial\bar{\omega}}\,d\bar{\omega}\,,$$

it is seen that the continuity equation (Eq. 18*) is identically satisfied. Upon elimination of the pressure P from Eq. 16* and 17*, along with the definitions of ψ, it can be shown that these equations reduce to

$$D\ (D - \frac{1}{\nu}\frac{d}{dt})\ \psi = 0. \qquad (20'^*)$$

where

$$D = \frac{d^2}{dx^2} + \frac{d^2}{d\bar{\omega}^2} - \frac{1}{\bar{\omega}}\frac{d}{d\bar{\omega}}$$

Stokes continues, "Since the operations represented by the two expressions within the parentheses are evidently convertible, the integral of this equation is

$$\psi = \psi_1 + \psi_2 \qquad (21^*)$$

where ψ_1, ψ_2 are the integrals of the equations

$$D\,\psi_1 = 0 \qquad (22^*)$$

$$(D - \frac{1}{\nu} \frac{d}{dt}) \psi_2 = 0." \tag{23*}$$

Then he shows that the change in pressure is given by

$$dP = \frac{\rho}{\bar{\omega}} \left(\frac{d^2 \psi_1}{dtdx} d\bar{\omega} - \frac{d^2 \psi_1}{dtd\bar{\omega}} dx \right) \tag{25*}$$

The transformation to polar coordinates (where

$x = r \cos\theta$, $\bar{\omega} = r \sin\theta$, $u = v_r \cos\theta - v_\theta \sin\theta$, and $q = v_r \sin\theta + v_\theta \cos\theta$)

reduces the above equations to

$$r \sin\theta \, (v_r \, r \, d\theta - v_\theta \, dr) = d\psi , \tag{26*}$$

$$\frac{d^2\psi_1}{dr^2} + \frac{\sin\theta}{r^2} \frac{d}{d\theta}\left(\frac{1}{\sin\theta} \frac{d\psi_1}{d\theta}\right) = 0, \tag{27*}$$

$$\frac{d^2\psi_2}{dr^2} + \frac{\sin\theta}{r^2} \frac{d}{d\theta}\left(\frac{1}{\sin\theta} \frac{d\psi_2}{d\theta}\right) - \frac{1}{\nu} \frac{d\psi_2}{dt} = 0, \tag{28*}$$

and

$$dP = \frac{\rho}{r \sin\theta} \left[\frac{d^2\psi_1}{dtdr} r d\theta - \frac{1}{r} \frac{d^2\psi_1}{dtd\theta} dr \right] \tag{29*}$$

where the stream function ψ is a function of r, θ, and t.

The position of the center of the inner sphere is given by δ, and Stokes made three more assumptions:

5. The velocity of the center is given by

$$\frac{d\delta}{dt} = \dot{\delta} = c \, e^{j\omega t} .$$

6. The stream function ψ is also periodic and of the form

$$\psi = p\, e^{j\omega t}$$

where p is a function of r and θ.

7. "....since the operation $\sin\theta \frac{d}{d\theta} \left(\frac{1}{\sin\theta} \frac{d}{d\theta} \right)$ performed on the function $\sin^2\theta$ reproduces the same function ...., it will be possible to satisfy equations (27*) and (28*) on the supposition that $\sin^2\theta$ is a factor of ψ_1 and ψ_2. Assume then $\psi_1 = f_1(r) \sin^2\theta\, e^{j\omega t}$, $\psi_2 = f_2(r) \sin^2\theta\, e^{j\omega t}$."

The substitution of

$$m^2 \nu = j\omega \tag{32*}$$

and the expressions for ψ_1 and ψ_2 into eqs. 27* and 28* gives

$$f_1''(r) - \frac{2}{r^2} f_1(r) = 0 \tag{33*}$$

$$f_2''(r) - \left(\frac{2}{r^2} + m^2\right) f_2(r) = 0. \tag{34*}$$

The boundary conditions for the viscous solution are

$$r = a \qquad v_r = \dot{\delta}\cos\theta \qquad v_\theta = -\dot{\delta}\sin\theta$$

and

$$r = b \qquad v_r = 0 \qquad v_\theta = 0$$

where $\dot{\delta}$ is the relative velocity of the inner sphere. From the relationships between the velocities and the stream function, these boundary conditions reduce to

$$f'(a) = ac, \; f(a) = \frac{1}{2} a^2 c \tag{35*}$$

$$f'(b) = 0 \quad , \quad f(b) = 0 \tag{36*}$$

where $f(r) = f_1(r) + f_2(r)$, a is the inner radius, and b is the outer radius. The solution to Eqs. 33* and 34* are

$$f_1(r) = \frac{A}{r} + Br^2$$

$$f_2\ (r) = Ce^{-mr}\left(1 + \frac{1}{mr}\right) + De^{mr}\left(1 - \frac{1}{mr}\right) . \tag{38*}$$

The resultant fluid force, F, acting on the sphere due to the pressure and shearing stresses of the fluid is given by

$$F = \pi \rho a \frac{d}{dt} \int_0^{\pi} \left\{ a \left(\frac{d\psi_1}{dr}\right)_a + 2 \left(\psi_2\right)_a \right\} \sin\theta \, d\theta \tag{49*}$$

which will yield

$$F = \frac{4}{3} \pi \rho a j\omega \left\{ a\ f_1'\ (a) + 2\ f_2(a) \right\} e^{j\omega t} \tag{50*}$$

when ψ_1 and ψ_2 are substituted and the indicated operations of integration and differentiation are completed.

For the case of two concentric spheres, Stokes substituted the relationship

$$Ka^2c = (-k + jC_s)\ a^2c = af_1'(a) + 2f_2(a)$$

into Eq. 50* where K $(= -k + jC_s)$ is a complex function. By noting the definitions of velocity and acceleration, F becomes

$$F = -(kM)\frac{d\dot{\delta}}{dt} - (M\omega C_s)\dot{\delta} \tag{27}$$

where M is equal to the mass of fluid displaced by the sphere. Recall that the relationship between G(t) and F is $G(t) = F + Mg + M\ du_o/dt$ from conclusion 1 of the potential flow solution. When this form of G(t) is substituted into Eq. 1-a, the differential equation of motion for the inner sphere is

$$(m_s + kM)\ddot{\delta} + (M\omega C_s)\dot{\delta} + K'\delta = F(t) + Mg + (M-m_s)\frac{du_o}{dt}\,. \tag{26-a}$$

XI. APPENDIX B. SUMMARY OF DATA

A. Series III

Fluid	Beam number	Stokes' number S_n	Added mass coefficient k	Fluid damping coefficient C_s
I	12	8.20×10^5	1.648	0.0323
IS	12S*	6.90×10^5	1.667	0.0388
I	9	4.60×10^5	1.525	0.0252
IS	9S	4.20×10^5	1.581	0.0324
I	4	2.00×10^5	1.480	0.0310
I	4R**	1.97×10^5	1.513	0.0333
V	12	1.75×10^5	1.665	0.0555
V	12S	1.77×10^5	1.699	0.0661
V	9	9.80×10^4	1.537	0.0610
V	9S	1.00×10^5	1.569	0.0657
V	4	4.30×10^4	1.485	0.0643
IV	12	2.00×10^4	1.748	0.1260
IV	12S	2.08×10^4	1.714	0.1240
IV	9	1.15×10^4	1.595	0.1500
IV	9S	1.18×10^4	1.618	0.1365
IV	4	5.02×10^3	1.733	0.2540
IV	4S	5.12×10^3	1.654	0.1965
III	12S	3.30×10^3	1.821	0.2690
III	9S	1.81×10^3	1.802	0.3570
III	4S	7.83×10^2	1.840	0.4440

*S means the moving support was supported at the center.

**R means the run was repeated.

B. Series V

Fluid	Beam number	Stokes' number S_n	Added mass coefficient k	Fluid damping coefficient C_s
I	12	6.50×10^5	1.697	0.0338
I	9	3.40×10^5	1.607	0.0274
I	9R*	3.40×10^5	1.603	0.0280
I	4	1.45×10^5	1.661	0.0490
V	12	1.29×10^5	1.715	0.0487
V	12RW**	1.44×10^5	1.715	0.0550
V	9	6.73×10^4	1.649	0.0493
V	9RW	7.64×10^4	1.646	0.0617
V	4	2.90×10^4	1.918	0.0968
V	4R	2.94×10^4	1.641	0.0870
V	4RW	3.34×10^4	1.672	0.1007
IV	12	1.32×10^4	1.750	0.2644
IV	9	6.81×10^3	1.759	0.1653
IV	4	2.94×10^3	1.790	0.3936
III	12	1.85×10^3	1.893	0.3640
III	9	9.50×10^2	1.913	0.4970
III	4	4.05×10^2	2.023	1.066

*R means the run was repeated.

**RW means the run was repeated with 454 gms attached at the center of the beam.

C. Series VI

Fluid	Beam number	Stokes' number S_n	Added mass coefficient k	Fluid damping coefficient C_s
I	12*	6.30×10^5	1.658	0.0305
I	9	3.30×10^5	1.590	0.0252
I	7	2.00×10^5	1.584	0.0283
I	4	1.40×10^5	1.584	0.0364
V	12*	1.26×10^5	1.690	0.0600
V	9	6.70×10^4	1.612	0.0561
V	7	4.00×10^4	1.616	0.0684
V	4	2.80×10^4	1.651	0.0896
IV	12*	1.33×10^4	1.745	0.1380
IV	9	6.60×10^3	1.690	0.183
IV	7	4.20×10^3	1.756	0.224
IV	4	2.90×10^3	1.803	0.284
III	12*	1.77×10^3	1.909	0.394
III	9	9.30×10^2	1.927	0.463
III	7	5.50×10^2	1.994	0.641
III	4	3.80×10^2	2.086	0.913

*These values for beam 12 were not plotted in Figs. 16 and 17.

D. Theoretical Values

Diameter ratio λ	Stokes' number S_n	Added mass coefficient k	Fluid damping coefficient C_s
0.7300	5.0×10^2	1.908	0.6702
0.7300	1.0×10^3	1.789	0.4334
0.7300	5.0×10^3	1.609	0.1713
0.7300	1.0×10^4	1.565	0.1176
0.7300	5.0×10^4	1.504	0.0506
0.7300	1.0×10^5	1.490	0.0354
0.7300	5.0×10^5	1.469	0.0157
0.7300	1.0×10^6	1.466	0.0109
0.7400	4.0×10^2	2.042	0.8451
0.7400	1.0×10^3	1.877	0.4691
0.7400	4.0×10^3	1.705	0.2085
0.7400	1.0×10^4	1.639	0.1262
0.7400	4.0×10^4	1.581	0.0607
0.7400	4.0×10^5	1.538	0.0187
0.7462	4.0×10^2	2.104	0.8926
0.7462	1.0×10^3	1.936	0.4936
0.7462	4.0×10^3	1.757	0.2184
0.7462	1.0×10^4	1.688	0.1320
0.7462	4.0×10^4	1.627	0.0635
0.7462	4.0×10^5	1.586	0.0195